UCRL 2806

UNCLASSIFIED

UNIVERSITY OF CALIFORNIA

Radiation Laboratory

TWO-WEEK LOAN COPY

This is a Library Circulating Copy which may be borrowed for two weeks. For a personal retention copy, call Tech. Info. Division, Ext. 5545

BERKELEY, CALIFORNIA

DISCLAIMER

This document was prepared as an account of work sponsored by the United States Government. While this document is believed to contain correct information, neither the United States Government nor any agency thereof, nor the Regents of the University of California, nor any of their employees, makes any warranty, express or implied, or assumes any legal responsibility for the accuracy, completeness, or usefulness of any information, apparatus, product, or process disclosed, or represents that its use would not infringe privately owned rights. Reference herein to any specific commercial product, process, or service by its trade name, trademark, manufacturer, or otherwise, does not necessarily constitute or imply its endorsement, recommendation, or favoring by the United States Government or any agency thereof, or the Regents of the University of California. The views and opinions of authors expressed herein do not necessarily state or reflect those of the United States Government or any agency thereof or the Regents of the University of California.

UCRL-2806
Unclassified Physics

UNIVERSITY OF CALIFORNIA

Radiation Laboratory
Berkeley, California

Contract No. W-7405-eng-48

THE MECHANISM OF THE REACTION $C^{12} + p \rightarrow p + 3\alpha$ AT 32 MEV

John Logan Need

(Thesis)

December 3, 1954

Printed for the U. S. Atomic Energy Commission

Contents

Abstract 3

Introduction 4

Experimental Procedures

- Beam Tube 9
- Collimation 9
- Intensity Monitor 11
- Magnet 11
- Cloud Chamber 11
- Photography 12
- Thermal Control 12
- Sequence of Operations 12

Analysis of the Data

- Details of the Measurements 14
- Beam Direction 17
- Errors in Measurement 17
- Calculations 22
- Identification Procedures and Acceptance of Events 24

Results and Comments 30

Acknowledgments 57

Appendices

- I. Range-Energy Relation 58
- II. Beam Energy 62

References 65

THE MECHANISM OF THE REACTION $C^{12} + p \rightarrow p + 3\alpha$ AT 32 MEV

John Logan Need

Radiation Laboratory, Department of Physics
University of California, Berkeley, California

December 3, 1954

ABSTRACT

A methane-filled expansion cloud chamber, operated at 1/3 atmosphere, was used to study the $C^{12} + p \rightarrow p + 3\alpha$ reaction. Two hundred events that satisfied momentum and energy conservation were accepted for analysis. One hundred forty-eight of these had all four prongs visible; the remaining fifty-two had only three visible prongs with the fourth prong directed into an invisible region of the chamber. There is no evidence for direct four-particle decay of N^{13*}. One-quarter of the events proceeded via the Be^{8} ground state and at least one-half via the 2.9-Mev level in Be^{8*}; possibly higher levels in Be^{8} were also involved. Evidence for the participation of levels in C^{12} at 9.6, 11.8, 16, 20, and 25 Mev was found. There are grounds for believing that the $C^{12}(p,\alpha)B^{9}$ reaction also participates with evidence for levels at 0 and 3.2 ± 1.0 Mev. The possibility of the $C^{12} + p \rightarrow Li^{5} + Be^{8}$ reaction was investigated and it was concluded that it could account for at most five percent of the events.

THE MECHANISM OF THE REACTION $C^{12} + p \rightarrow p + 3\alpha$ AT 32 MEV

John Logan Need

Radiation Laboratory, Department of Physics
University of California, Berkeley, California

December 3, 1954

INTRODUCTION

One of the first successful analyses of a nuclear reaction in which the reaction products consisted of more than two particles was that of Dee and Gilbert[1] explaining the alpha-particle energy spectrum from B^{11} (p, α) Be^{8}. Three alpha particles are produced in this reaction and (for 200 kv protons) they fall into three groups:[2]

1. A homogeneous group at about 5.7 Mev.
2. A broad group at about 3.85 Mev.
3. A continuous distribution extending from low energies to about 5 Mev, which contains roughly twice as many particles as Group 2.

According to Dee and Gilbert, Group 1 is due to the reaction $B^{11} + p \rightarrow \alpha + Be^{8}$ with the Be^{8} formed in the ground state. It contains only about 1 percent of the alpha particles.

Group 2 is produced by the reaction $B^{11} + p \rightarrow \alpha + Be^{8*}$ and yields a value of 2.8 Mev for the excitation energy of the Be^{8*} nucleus. This group is not monoenergetic and has a width at half maximum of 0.51 Mev, which gives a width of 0.77 Mev for the Be^{8} excited level.

Group 3 is then due to the breakup of the excited Be^{8*} nuclei, $Be^{8*} \rightarrow 2\alpha$. For constant bombarding energy and a unique excitation of the Be^{8} nucleus, both the velocity of the Be^{8*} (v_{Be}) in the center of mass and the velocity of the second and third alpha particles (V_{α}) in the Be^{8*} rest frames are constants. The energy of the second and

third alpha particles in the center of mass is then given by

$$E_\alpha = \frac{m}{2} v_\alpha^2 = \frac{m}{2}(v_{Be}^2 + V_\alpha^2 - 2v_{Be}V_\alpha \cos\theta),$$

where θ is the angle between the direction of flight of the Be^{8*} nucleus and the direction of the breakup of the Be^{8*}. Assuming isotropic breakup in the Be^{8*} rest frame,

$$dN/d\Omega = \text{const.} = dN/2\pi \sin\theta\, d\theta.$$

Now, by differentiating the expression for E_α, we get

$$dE_\alpha/d\theta = 2v_{Be}V_\alpha \sin\theta = \text{const.} \sin\theta.$$

Therefore

$$dN/dE_\alpha = \frac{dN}{d\theta}\bigg/\frac{dE_\alpha}{d\theta} = \frac{2\pi \sin\theta \cdot \text{const.}}{\text{const.} \cdot \sin\theta} = \text{const.}$$

or, the distribution in energy of the second and third alpha particles is uniform in the center of mass. The agreement between the experimental and calculated spectra was excellent.

In 1949, Hänni, Telegdi, and Zünti[3] observed three-prong stars in nuclear emulsions that had been exposed to the γ-rays from protons on lithium. They determined the sum of the energies of the three prongs for each event (E_t), assuming them to be alpha particles. The distribution in E_t showed two peaks, one at 7.5 Mev and the other at 10.1 Mev. These values are in agreement with the known energies of 17.6 and 14.8 Mev for the lithium γ-rays and the value of 7.4 Mev for the Q of the $C^{12}(\gamma, 3\alpha)$ reaction. These stars were therefore identified as being due to this reaction produced in the carbon present in the emulsion.

The energy spectrum of the alpha particles from the stars due to the 17.6-Mev γ-ray showed a continuum which went to 5.3 Mev and showed a marked peak at 4.7 Mev. This spectrum is similar to that obtained by Dee and Gilbert from the reaction $B^{11} + p \rightarrow 3\alpha$. The analysis was carried out in the same fashion and yielded similar results, i.e., a

two-step process, in which the first step is a $C^{12}(\gamma,\alpha)Be^{8*}$ reaction where the Be^{8*} nucleus is left with an excitation energy of 3.0 Mev, and the second the breakup of the Be^{8*} into two alpha particles. They also noted stars that were interpreted as going through the ground state of Be^{8}.

Following this, many experimenters[4-11] have investigated the $C^{12}(\gamma,3\alpha)$ reaction at γ-energies up to 300 Mev. Their results can be summarized as follows:

Energy Dependence of the Cross Section:[5-8, 10, 11] The cross section as a function of energy shows two large peaks at γ-energies of 19 and 29 Mev, with a marked minimum at 21 Mev. No events have been observed at energies above 42 Mev. Examination of some 2,500 stars gives evidence that the two peaks are formed by the superposition of narrow resonances spaced at about 1-Mev intervals. The strongest of these lie at γ-energies of 17.3, 18.3, 21.9, 24.3, 26.5, and 29.4 Mev. The presence of these multiple resonances and the strong minimum in the region of the giant (γ, n) resonance suggest a definite compound-nucleus reaction.[8]

Reaction Mechanism:[4-10] At an energy of 17.6 Mev the reaction proceeds predominantly via the 3.0-Mev level in Be^{8*} with about two percent going via the ground state. This preference for the 3.0-Mev excited level holds true for γ-energies below about 19 Mev. For stars due to γ-energies greater than 26 Mev the reaction seems to proceed via either the ground state in Be^{8} (12%) or one of three levels in Be^{8*}, at 16.9, 17.8, or 16.4 Mev, with the 16.9-Mev level predominating. This level has J=2 and even parity, and is possibly the analogue of the Li^{8} and B^{8} ground states with the isotopic spin T=1.

In the region between 19 and 26 Mev the mechanism of the reaction is uncertain. The proportion of events that go via the ground state of Be^{8} increases with energy from about 5% to 18% in this region.

Those events which go via the 3.0-Mev level in Be^8 can account for at most one-third of the events. It may be that higher levels in Be^8 are involved, or possibly even three-particle breakup in the remainder of the events. The present data are inconclusive on this point.

The breakup of C^{12} into three alpha particles has also been initiated by neutrons. Aoki[12] noted three-prong stars in a methane-filled cloud chamber exposed to Li+D neutrons. Their total energies were in agreement with the assumption of the reaction C^{12} (n, n') 3α. Most of the stars showed a random distribution of energy among the prongs, but there were some that had two short prongs and the other quite long. These have since been interpreted as events that went through the Be^8 ground level.

In 1949, Green and Gibson[13] exposed nuclear emulsions to neutrons from deuterons on lithium and observed three-prong stars. The stars were not seen when the neutron energy was below 7 Mev. At the energies available the two possible reactions were

$$N^{14} + n \rightarrow Li^7 + 2\alpha - 8.8 \text{ Mev},$$

$$C^{12} + n \rightarrow n' + 3\alpha - 7.4 \text{ Mev}.$$

The stars were analyzed to obtain the energies of the incident and scattered neutrons. The observations were sufficiently accurate to eliminate the possibility of the nitrogen reaction, and the stars were therefore identified as being due to the C^{12} (n, n') 3α reaction.

The data of Green and Gibson were analyzed further by Livesey and Smith[9], who found that the energy spectrum of the inelastically scattered neutrons showed two peaks corresponding to energy levels in C^{12} at 9.6 and 11.8 Mev. Those events which appeared to go via the 9.6-Mev level in C^{12} were all consistent with the assumption that they involved the ground state of Be^8. The events that corresponded to the 11.8-Mev level in C^{12} went via the broad 3.0-Mev level in Be^{8*}.

In the experiment discussed herein methane was bombarded with 32-Mev protons in order to study the $C^{12} + p \rightarrow p + 3\alpha$ reaction. It was expected that many of the above-mentioned features of the reaction mechanism would show up in the work. An investigation of this reaction is made difficult by the presence of three competing reactions, which yield the same end products and give the same appearance in a cloud chamber. The three possible reactions are

1. $C^{12}(p, p')C^{12*} \rightarrow Be^{8} + \alpha \rightarrow 3\alpha$,
2. $C^{12}(p, \alpha)B^{9} \rightarrow Be^{8} + p \rightarrow p + 2\alpha$,
3. $C^{12}(p, Li^{5})Be^{8} \rightarrow p + 3\alpha$.

Reaction 1 is suggested as parallel to the $C^{12}(\gamma, 3\alpha)$ and $C^{12}(n, n')3\alpha$ reactions in which C^{12} is formed in an excited state as an intermediate nucleus. The first step of the second reaction has been identified at a bombarding energy of 18 Mev.[14] Peaks in the alpha-particle spectrum corresponding to the ground and first excited levels of B^{9} were seen together with a large background of alpha particles at low energies. Reaction 3 is included as being energetically possible, although difficult to identify.

If the reaction proceeds by way of one or more levels in C^{12} one may expect the proton energy spectrum (in the center-of-mass system) to show peaks at energies corresponding to the levels involved. Similarly for those events which go by way of B^{9} the energy spectrum of the alpha particles should show peaks.[14] Finally, in Reaction 3, there should be peaks in the energy distribution of the Be^{8*} (calculable, although not directly observed) according to whether the Li^{5} and the Be^{8} are in their ground or excited levels.

EXPERIMENTAL PROCEDURE

Beam Tube

The cloud chamber was operated in the annex of the linear accelerator building. A plan view of the arrangement is shown in Fig. 1. The proton beam from the linear accelerator was deflected 10° by the steering magnet (C) and sent down a 25-foot evacuated tube to the chamber. The last 10 feet of the beam tube was made of soft iron pipe with a 2-inch outside diameter and 0.25-inch walls. This was done so that the beam diameter was not greatly increased through deflection and momentum analysis of the beam by the fringing field of the Helmholtz coils. To keep the iron pipe from deflecting when the magnetic field came on, it was fastened to a rigid aluminum A-frame which was cast in a heavy concrete base. A 0.001-inch aluminum thin window covered the end of the beam tube.

Collimation

Three collimators were used: The four-jaw collimator (B) at the exit end of the linear accelerator; a carbon collimator (D) with a diameter of 0.1 inch, placed at the exit of the steering magnet; and a carbon collimator of 1/8-inch diameter at a distance of 15 feet along the beam tube from (D), shadowed by a carbon clipper of 5/32-inch diameter placed 1 foot away. The four-jaw collimator was used to limit the intensity of the beam entering the chamber. The maximum beam intensity available in the annex was about 1000 times too great for usable pictures. During the initial tune-up and steering the four-jaw collimator was left open to facilitate the process of getting maximum beam at the cloud chamber, and then adjusted to give the proper number of protons to produce two or three events per picture. The carbon collimators defined the beam direction and diameter.

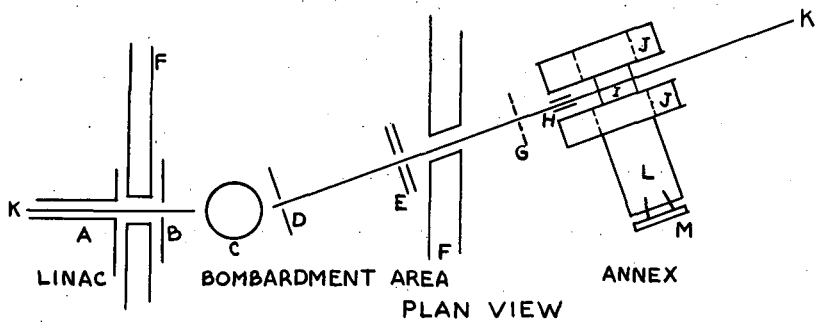

A HIGH ENERGY END OF LINAC
B 4 JAW COLLIMATOR
C STEERING MAGNET
D PRIMARY COLLIMATOR
E SECONDARY COLLIMATOR AND CLIPPER
F WALLS OF BUILDING
G THIN WINDOW AT END OF BEAM TUBE
H ION CHAMBER
I CLOUD CHAMBER
J HELMHOLZ COILS
K PROTON BEAM
L CAMERA TUBE
M STEREOSCOPIC CAMERA

MU-8025

Fig. 1. Plan view of the experimental geometry

Intensity Monitor

Between the end of the beam tube and the chamber an air ionization chamber was placed to permit the operator to adjust the machine between pulses for maximum beam intensity. An air chamber with no windows was chosen to give minimal stopping power.

Magnet

The air-cooled Helmholtz coils (J) produced a peak field of 6870 gauss with a current of 2200 amperes when used in pulsed operation. Current was supplied by a 540-kw minesweeper generator with a 2-ton flywheel mounted between the motor and generator. The current pulse, synchronized with the cloud-chamber cycle, had a rise time of 2-1/2 seconds and remained stationary at its peak for about 0.2 second. A cycle time of about 2 minutes was used. This limit was imposed by the maximum temperature at which the magnet could be safely operated.

Cloud Chamber

The cloud chamber (I) was generally cylindrical in shape and was operated with its axis of rotation horizontal. It consisted of front and back volumes of 15-inch inside diameter, the front volume being 4 inches high and the back volume 5 inches. The beam entered the chamber through a thin window of 0.001-inch aluminum. Front and back volumes were separated by a lucite piston sealed by a diaphragm of 1/32-inch gum rubber. Pantograph arms were used to keep the piston parallel to the front glass during the expansion. Black velvet over a cheesecloth pad covered the piston on the front volume side. This was used as a black background for the photography and as a wick to supply water vapor to the top of the chamber. A clearing field was maintained between the piston and a grid of 3-mil tungsten wire mounted on a lucite spacing ring just back of the front glass. Fiducial marks of known separation were scribed on the inside of the front glass.

Since it was desired to operate at a total pressure of about 1/3 atmosphere, a cylindrical tank 13 inches in diameter and 17 inches long was put over the pop valve and evacuated to a pressure of about 100 microns before each expansion. When the pop valve was opened the pressure in the back volume dropped to about 1/9 atmosphere, which permitted the pressure in the front volume to expand the chamber. The back-volume air pressure was controlled by a Moore regulator which used a vacuum as the reference pressure. Compressed air was used at the input to the Moore regulator to give a sufficiently fast compression. Slow expansions were obtained by the use of a solenoid valve which simultaneously connected the back volume to the vacuum tank and turned off the back-volume air supply.

Photography

Stereo pairs were taken with a specially constructed stereoscopic camera (M) mounted 54 inches from the front glass of the chamber at the end of a lighttight box. The pictures were taken on 100-foot rolls of Eastman Linagraph Ortho film with a matched pair of Wollensak Velostigmat 127 mm lenses operated at f 8. Illumination was by means of two General Electric FT422 flash tubes. Each tube was connected across a 256-microfarad capicator bank which was charged by a 2000-volt power supply. The discharge was initiated by a high-voltage pulse from a spark coil (triggered as described below).

Thermal Control

Both the inside faces and the cylindrical holes of the two magnet coils were supplied with heat shields. Tap water was run through these to insulate the chamber from the heat of the coils. A box was constructed around the chamber and beam-tube assembly in the space between the two magnet coils to keep room air from blowing on the front volume of the chamber. The camera tube sealed the front of the

chamber and the back plate sealed the rear. A small, high-speed blower, mounted with the motor outside the box, was used to circulate air in the region between the coils. It was necessary to introduce warm air from a hair dryer into the camera tube to keep the front glass from fogging. The temperature inside the chamber was measured indirectly with a mercury thermometer placed in a jar of water in the box between the coils.

Sequence of Operations

The linear accelerator was operated at a repetition rate of 15 pulses per second. Each pulse was 600 μsec long. Synchronization with the cloud chamber equipment was effected by means of the linear accelerator equipment pulse, which preceded the beam by about 20 μsec.

Fifteen seconds before each expansion the beam was turned off by shifting the ion-source pulse out of phase with the rf acceleration. At the end of the waiting period first the field and then the contactor of the generator was energized and a variable time delay started. The ending of the delay cocked the fast timer, which was then initiated by the next incoming equipment pulse. The fast timer turned off the clearing field, initiated the fast expansion, fired the lights, and turned off the generator field. It also selected the one equipment pulse on which the ion source was shifted back into phase. In addition, a signal was obtained when the cloud chamber piston hit bottom. The timing of the fast sequence was recorded on paper tape, which permitted rapid adjustment of the timing. The sequence was set to bring the beam into the chamber 4 milliseconds after the piston hit bottom and to flash the lights 33 milliseconds after the beam had entered.

At the end of the fast-timer sequence the linear accelerator beam was turned on to permit the operator to adjust for maximum beam. A pneumatically operated lead shutter prevented the beam from entering the chamber during this time. Two slow expansions were used, followed by a waiting period of 50 seconds until the beginning of the next cycle. During the slow expansions the clearing field was turned on and the magnet contactor opened.

ANALYSIS OF THE DATA

After development, the film was scanned under a high-power stereoscopic viewer, and all events that appeared to consist of three or more concurrent tracks were listed. A sketch of the appearance of each event was made. The film was then put in the projection apparatus, which duplicated the geometry of the camera optics and produced full-sized images of the tracks on a translucent screen (Fig. 2). Two Western Electric 300K zirconium arc lamps provided illumination. Because of the way the projection apparatus was set up the axis of the cloud chamber, which had been horizontal during the experiment, was vertical in projection.

Details of Measurement

The translucent screen was placed in a horizontal position at a height such that it was the same distance from the lenses of the projection apparatus as the back of the front glass had been from the camera lenses. The position of the film and the focus were adjusted until the sets of images for each of the two fiducial marks coincided and the separation between the images of the two fiducial marks was equal to the separation of the two fiducial marks on the front glass. The table was then raised until some point near the beam on one track of the event was coincident on the screen at an arbitrary point along the horizontal axis AA. Rotating the screen about the horizontal axis AA (with AA approximately normal to the track) brought the two images of the entire track into coincidence. The origin of the table was then moved to the estimated position of the origin of the event and adjusted in height until the track images were again coincident. With its height kept unchanged, the table was rotated about a vertical axis until the line BB was along one of the other tracks of the event and then it was determined whether the entire track could be brought into coincidence

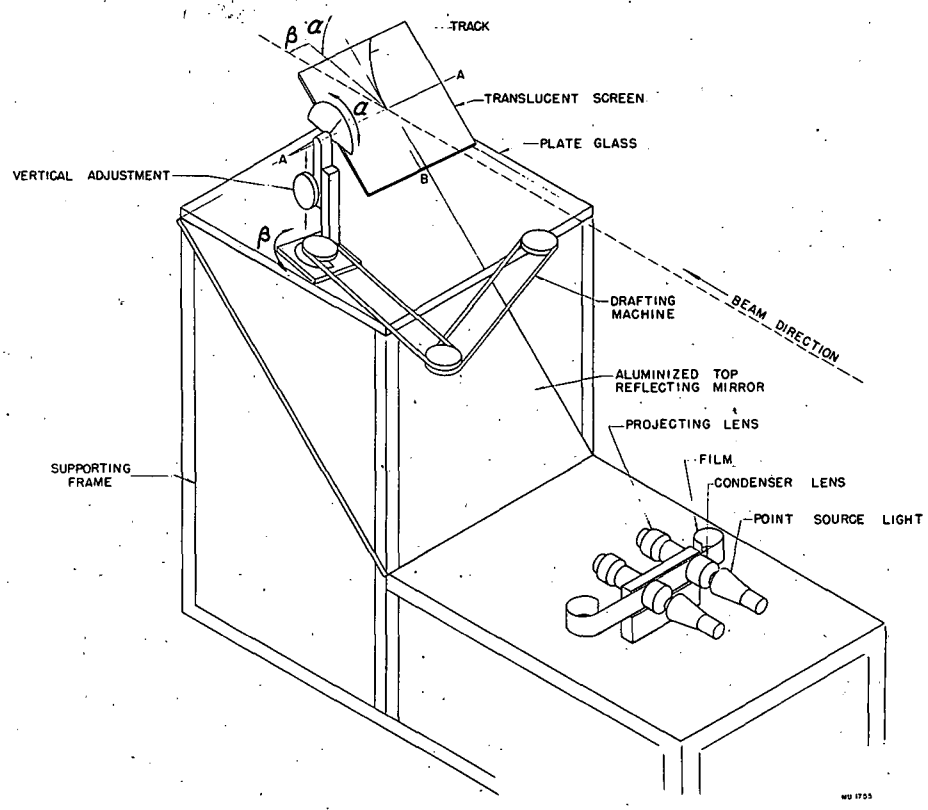

Fig. 2. Diagram of projection apparatus.

by merely rotating the translucent screen about AA. If all the tracks apparently belonging to one event could be brought into coincidence at the same height, data on the event were recorded.

The raw data were recorded on Keysort cards, one card per track. For each event the following items were recorded: picture number, identifying letter, number of prongs, gas mixture, and "origin". The "origin" is the distance, measured along the beam, of the origin of an event from an arbitrarily fixed point in the chamber. For each track the following measurements were made:

The dip angle α (degrees): the angle in the vertical plane between the tangent to the track at the origin and the horizontal plane.

The slant radius of curvature ρ_s, or the range R (cm). R was measured if the track ended in the visible portion of the chamber. Sometimes both ρ_s and a minimum value for R were recorded when a track had the appearance of ending soon after leaving the chamber.

The beam angle β_M (degrees): the angle, in the horizontal plane, between the vertical plane through the tangent to the track at the origin and an arbitrarily fixed direction in the horizontal plane.

For those tracks where ρ_s was measured the following additional data were recorded:

The distance D (cm) from the center of the measured portion of the track to the center of the chamber.

The percentage error in ρ_s, determined from the length of the chord of the measured portion of the track and the assumption that the error in reading the sagitta is 0.10 mm, independent of the curvature.

The angle α is the angle, measured from the horizontal, through which the screen had to be rotated about AA to bring the two images of the track into coincidence. The slant radius of curvature was measured by matching the curve with one of a series of arcs ruled on a lucite template. A line ruled on the template perpendicular to all the arcs was placed along AA with the chosen arc tangent to BB, and the screen was then rotated about a vertical axis until the arc and the image of the track lined up. The angle β_M was read on a divided circle on the head of the drafting machine.

Beam Direction

Because the direction of the beam changed as it went across the chamber, the angle β_M measured for each track had to be corrected to obtain the angle β, where β is the angle (measured in the horizontal plane) between the vertical plane through the tangent to the track at the origin of the event and the beam direction. Figure 3 shows a schematic of the angles. From the values of s and β_B obtained for the beam-energy determination, as described in Appendix II, the variation of the beam direction with the position along the beam was found. The average values of 28 determinations of β_B for each of 14 points along the beam were plotted against s, and a straight line was fitted to the points. The probable error of each point was $\pm$ 0.7°. Using this graph and the value of the "origin" for each event the value of β_B appropriate to the event was found.

Errors in Measurements

Range. The sources of error in the energy as measured by range were: the range-energy relation, straggling, and the determination of the origin of the event. The error in the range-energy relation as discussed in Appendix I, was $\pm$ 5%. In the case of straggling, the average error was $\pm$ 2 mm. The uncertainty in the position of the origin was taken to be

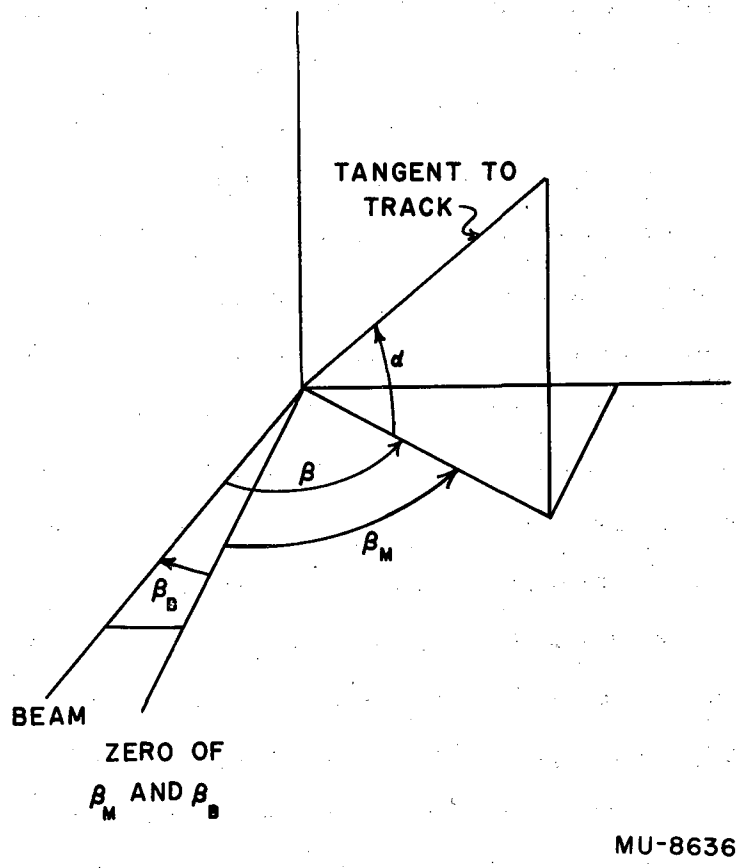

Fig. 3. Schematic defining the angles used in measurements.

2 mm. This uncertainty was due to the fact that the origin was hidden by the beam, so that its position had to be determined by projecting the prongs of an event back to their intersection.

Magnetic Field. The magnetic field strength was determined by recording the peak current of each pulse during the running time of the experiment. After the experiment the field was measured with a search coil and integrator. The measuring equipment was synchronized to measure the field at that time in the cloud chamber cycle at which the proton beam entered the chamber. Measurements were taken throughout the volume occupied by the chamber. The search coil and associated equipment were calibrated in a test field that had been measured by means of the proton magnetic moment. Thus the results obtained express the magnetic field in terms of current readings taken on the same ammeter and in the same fashion as during the experiment. The quoted inaccuracy in the field measurement was $\pm$ 0.3%.

The field was found to be cylindrically symmetric in the cloud chamber volume, and the axial variation over the illuminated region was less than 1%. A plot of magnet current vs magnet field at the center and a plot of the radial variation of the field (the field at the center being 100) were made and used to obtain the magnetic field at the center of the portion of the track used for the radius-of-curvature measurement. The error in $B\rho$ due to the magnetic field was about 1%, which is small compared to the errors due to the curvature measurements.

Radius of Curvature. Measurements carried out in the cloud chamber group here over the past several years have shown that the error made in matching the arcs ruled on the templates to the tracks amounts to

0.1 mm in the sagitta, independent of the curvature and track length available. A nomograph was constructed which gave the percent error in ρ_s as a function of ρ_s and L, the length of the track used for measurement. The relation connecting the variables is $\delta \rho_s = 100\, \Delta\rho_s / \rho_s = 8\, (\rho_s / L^2)\, (1 + 0.08\, \rho_s / L^2)$.

Another source of error was the curvature C_t, due to multiple scattering and turbulence. To determine this curvature, pictures were taken with no field and a weak beam. Measurements of 24 tracks were made with a precision comparator microscope. The curvatures were determined by plotting the tracks with the transverse scale magnified by a factor of 100, drawing in the curves, and measuring the sagittae and lengths. The distribution in curvatures yielded a mean value of $C_t = 1/(25\text{m})$. The average track had a radius of 50 cm and a $\delta\rho_s$ of 8%. Therefore the error ($\sim$2%) due to turbulence and multiple scattering was negligible with respect to the measurement errors.

Angular Measurements. The accuracy of the angular measurements with the equipment used has been thoroughly investigated by Wilson Powell et al.[15] They found that the angle α was reproducible to within $\pm 1^\circ$, and the angle β_M to within $\pm 1.5^\circ$, for cases in which the origin of the event was visible. The origins of the events were not visible in this experiment. My experience has indicated that the best estimate for the error in β_M is $\pm 2^\circ$, while the error in α is best represented by the relation $\delta\alpha = 0.035\, (1 + \alpha)$, where α and $\delta\alpha$ are in radians.

The error in the measurement of α is due to the uncertainty in the determination of the heights of the end points of the tracks, and is therefore approximately proportional to 1/L. The increase in error in α at larger angles was chiefly due to the shift in the origin caused

by refraction as the translucent screen was rotated, and to the consequent uncertainty as to the position of the origin.

Because the origin of the event was not visible and the track had to be projected back to the origin, there was an error in β_M caused by the error in ρ_S. Let β_e be the angle that the track has at the visible edge of the beam, then $\beta_M = \beta_e + L/\rho_S$, where β_M is the angle at the origin of the event, L the distance along the track from the edge of the beam to the origin of the event, and ρ_S the slant radius of curvature of the track. If primes denote measured quantities, then one can obtain from the above equation

$$\beta_M - \beta_M' = L(\rho_S - \rho_S') / \rho_S \rho_S'$$

or

$$\Delta\beta_M = L \, \Delta\rho_S / \rho_S^2.$$

For a typical track, L = 3 cm; ρ_S = 50 cm; and $\Delta\rho_S$ is 8% of 50, or 4.0 cm. This gives a typical error in β_M of 0.3°. For short stubs the uncertainty in ρ_S was quite large, and therefore the error in β_M for tracks of from 1 to 4 cm was estimated to be as high as ± 8°.

There is an additional uncertainty in β (as differentiated from β_M) because of the uncertainty in the direction of the beam at the position of the event. As discussed under "Beam Direction" in this chapter, the probable error in the determination of the beam direction was ± 0.7° at each point. The radius of curvature of the proton beam in the field was 114 cm. This was sufficiently great that an error of 3 mm in the position of the origin of the event produced a negligible error in the direction of the track with respect to the proton beam.

Deflections that occur before the particles emerge from the opaque region of the beam would result in errors in α and β, and, if sufficiently large, would upset the energy and momentum balance of the event. The probability that a typical (6 Mev) alpha

particle would suffer a single scatter of $2\text{-}1/2^{\circ}$ or more in a distance of 3 cm is about 0.003. The rms deflection due to multiple Coulomb scattering for the same particle is 1.2°.

The typical angular errors were used in the calculations except for those cases in which the track was exceptionally short or badly obscured. For the latter the estimated errors were used.

Rereading of the Film. As a check on the author's measurements the film was read a second time, and where discrepancies greater than the expected errors were noted, the film was read a third time. For those values which were read three times, adjustments were made, sometimes in the values themselves, and sometimes in the errors ascribed.

Calculations

These calculations were preliminary to the acceptance of an event:

Tracks for which R was measured. The energy was obtained from the range-energy graph appropriate to the mixture. The momentum was calculated from the relations $P = \sqrt{E}$ for alpha particles and $P = 0.502\sqrt{E}$ for protons. (The unit of momentum was taken to be the momentum of a 1-Mev alpha particle.) Next, the rectangular components of the momentum were calculated from

$$P_X = P \cos\alpha \sin\beta ,$$

$$P_Y = P \sin\alpha ,$$

$$P_Z = P \cos\alpha \cos\beta ,$$

the z direction being taken along the beam and the other two perpendicular to the beam direction.

Tracks for which ρ_s was measured. From the picture number and D, the magnetic field at the center of the measured portion of the track was determined, using tables calculated from the magnetic field measurements. The value of $\rho = \rho_s \cos \alpha$ was then determined and the product $B\rho$ found. The value of the energy in Mev was determined from an alignment chart which represented the function $B\rho = 10^4/3 \times \sqrt{E(E + 1876)}$. The same chart was used for both protons and alpha particles. The momentum was obtained from the relations $P = 3.47 \times 10^{-6} B\rho$ for protons and $P = 6.94 \times 10^{-6} B\rho$ for alpha particles. Finally, the rectangular components of the momentum were calculated as above.

Special cases. For those tracks where both ρ_s and R were measured the calculations were carried out through the energy determinations. Then the energies were compared. These tracks were those that did not have the appearance of ending in the illuminated region of the chamber but rather had the appearance of ending soon after leaving the illuminated region. In these cases R is the length of track visible and yields a minimum value for the particle energy. Generally the energy as determined by R was less than that determined by ρ_s, as was expected. However, there were cases where the energy as measured from R was greater than that determined from ρ_s. These cases were alpha particles with dip angles greater than 45°, for which the curvature was made indeterminate by a narrowing of the track image at both ends of the track. Next to the beam this narrowing was due to the paucity of water vapor available for drop formation because of the high density of ionization in that region. At the other end, the narrowing was due to the weakening of the illumination as the particle left the illuminated region. For these cases the energy was taken to be the energy determined from the range, and the error in the energy to be 15%.

When the identification of a particle was in doubt the calculations were carried out on the basis of both assumptions.

Propagation of errors. In order to determine a quantitative acceptance criterion for an event, it was necessary to calculate the error in the components of the total momentum. To obtain these values for each event the errors in measurement for each track were combined and propagated, assuming the errors in α, β, and ρ_s (or R) to be independent. For ease of computation, the error propagation was done by using percent errors. Tables were constructed from which the percent errors in the several momentum components could be determined. The tables were triple-entry tables which gave δP_i for various values of α, β, and δP. The maximum error in the interpolation in the tables was about 5%. The probable errors in the momentum components were then obtained by multiplying the value of the component by the percent error in that component.

Identification Procedures and Acceptance of Events

Each event read was identified as being a three-, four-, or five-prong event according to the number of visible prongs. In order to separate those events caused by the C^{12} (p, p') 3α reaction from all the three-, four-, and five-prong events read, the following identification procedure was used. The events of interest consist of four prongs; one--the proton--being lightly ionizing and the other three--the alpha particles--having much greater ionization. Furthermore, the total energy of the event is equal to the beam energy less the reaction energy, and the total momentum is equal to the incident momentum. Of course there may be some cases wherein the particle identification is uncertain because of chamber condition or when the prong has a range of less than about 3 cm.

There were seven five-prong events consisting of a proton and four alpha particles, which were identified as being examples of the O^{16} (p, p') 4α reaction in the oxygen present in the water vapor. The total prong energies of each of these events ($\sim$14 Mev) were consistent with the identification, and the momentum balance was satisfactory. The alpha prongs were short, about 3 to 4 cm, so that one could easily be hidden by the opaque region of the beam. Therefore, those four-prong events which did not balance in longitudinal momentum and for which the total energy was about 14 Mev had to be investigated for the possibility that they were in fact oxygen events with the fifth prong hidden by the beam.

Among the four-prong events there were some that did not have the proper appearance. They had two lightly ionizing prongs. These events were investigated in the high-power stereoscopic viewer, and most of them were identified as the overlap of two elastic p-C scatters. In the five remaining events, one of the two lightly ionizing prongs was discarded and the event was calculated as a three-prong event. Subsequent calculations disposed of three of them.

The remainder of the four-prong events, 211 in all, were tested for energy and momentum balance, to determine whether they were the C^{12} (p, p') 3α reaction. Where the identification of one or more prongs of an event was in doubt, that choice of identity was made which gave three alphas and one proton together with the smallest deviation from momentum balance. Furthermore, if the momentum balance could be improved by interchanging the particle identities of two of the prongs of an event, it was done. All the identities obtained by this requirement of best momentum balance were checked in the high-power stereoscopic viewer by another observer, and if the ionization did not check with the identity chosen, the event was not accepted. Only two events where the

identity of two particles had been interchanged were accepted. Of those events where the initial particle identification was uncertain, eight were accepted.

Of the 211 events with four prongs visible that were assumed to be carbon events, 135 were accepted after the first balance. The remainder of the events were examined to see if any of them could be identified as oxygen events. A fifth prong was fabricated which balanced the momentum. The requirements for acceptance as an oxygen event were that this prong be directed into an invisible portion of the chamber and that the total energy of the event be about 14 Mev. Ten events met these requirements. The total number of oxygen events (17) is in agreement with the number expected from the amount of oxygen present in the chamber.

One event was identified as a C^{13} (p, d) 3α reaction. The deuteron track had a radius of curvature equal to that of the beam, but with a density of ionization three times that of a beam proton. When it was identified as a C^{12} event, the total energy was greater than the beam energy; but when it was identified as a C^{13} event, the total energy was correct. Two other events were identified as possibly due to this reaction.

Those events left over, i.e., those not identified, were re-examined under the high-power stereoscopic viewer with the data cards at hand. More detail was visible in the viewer than was visible on the projector because a greater intensity of illumination was available. Each event was examined carefully to see if any reason could be found either to discard it or to adjust the data so that it would become acceptable. These reasons included excessive turbulence, possible overlap of two events, improper choice of the fourth prong when more than four prongs came from the same region, and a scatter that could change the measurement of the radius of

curvature. Further, the cards were re-examined to see what adjustments were necessary to bring the event into balance. Fifty-four events were discarded for one or more of the above reasons, but there were 23 that had the appearance of being good events. So that personal prejudice could be avoided, these events were reread by another member of the group. The result of this final examination was that only 5 of the events became acceptable. Of the others, 15 had momentum deviations that were outside the acceptable limits but still within twice these limits, i.e., they were probably true C^{12} (p, p') 3α events rejected by the acceptance criteria.

The four-prong events were accepted on the basis of momentum and energy requirements. For each event the X, Y, and Z components of the total momentum were found. Properly, the X and Y components of the total momentum should have been zero and the Z component equal to the momentum of the incident proton (2.70 in the units used). An event was not accepted if the deviation from the proper value of any one of the three components of the total momentum was greater than the sum, over the prongs of the event, of the errors in that component. Further, those events were rejected for which the total energy differed from 21.6 Mev by more than the sum of the errors in the prong energies. (This value is equal to the beam energy less the reaction energy of 7.4 Mev for the $C^{12} \rightarrow 3\alpha$ reaction.) The simple sum of the errors was used, rather than the correct square root of the sum of the squares, for the sake of ease in computation. The simple sum lies between one and two times the value of the square root of the sum of the squares, and was considered to be a satisfactory criterion for selection.

For each of the 138 events with three visible prongs a fourth prong was fabricated to give perfect momentum balance. The events were accepted when the following requirements were met: (a) the

deviation from 21.6 Mev of the sum of the energies of the four prongs was less than twice the sum of the errors in the energies of the three measured prongs; (b) the fabricated prong was directed into an invisible region of the chamber; and (c) the invisible particle was chosen so that the event had one proton and three alpha particles. Those three-prong events which met the energy requirement, 60 in all, were then examined under the high-power stereoscopic viewer to determine whether the prongs would or would not have been visible were they at the angles computed. Forty-six were accepted as bona fide C^{12} (p, p') 3α events, since the fourth prong, as calculated, would not have been seen.

Because of the greater visibility into the opaque region when the film was viewed on the stereoscopic viewer, there were 14 additional events for which the fourth prong was found where computed. In six of these cases only the angles of the fourth prong could be read; it was impossible to make a reasonable estimate of the momentum. The momentum was chosen to give the minimum value of the sum of the deviations from momentum balance. For the remaining eight events it was possible to get all the measurements on the fourth prong and therefore these eight events were then considered as four-prong events. They were all acceptable. Of the three-prong events that did not meet the energy requirement, the great majority had an energy around 15 Mev. However, no attempt was made to identify them.

The total number of events accepted was 200. One hundred and forty-eight of them had all four prongs visible; the other 52 had three prongs visible and the fourth calculated to be in the invisible region of the chamber. In order to check whether the three-prong events that were accepted had the same characteristics as the four-prong events, the average value of total energy of an event was determined for each group. The average total energy of a four-prong event was 21.9 Mev

and that of a three-prong event was 21.7 Mev, which is in very good agreement. However, there were differences between the two groups that showed up later in the investigation. There were very few events among the three-prong group that had a high-energy alpha particle--only three out of 52, as compared to 55 out of 148 for the four-prong events. Also, the proportion of three-prong events decreased for higher excitation energies in C^{12}, with 32 ± 7% in the 8.0-to 17.0-Mev group and 21 ± 5% above that. The shorter a track, the larger the solid angle for which it would be hidden by the beam; and these shorter tracks would be produced in the events where the proton or one alpha particle took away most of the energy.

RESULTS AND CONCLUSIONS

The first possibility to be checked was that of a direct four-particle breakup of the N^{13*} compound nucleus. This was done by plotting the energy distribution of the alpha particles in the center-of-mass system. The transformation to the center-of-mass system was carried out with the assumption that the incident proton had an energy of 28.9 Mev. If the reaction goes by way of a four-particle breakup, then the distribution in energy of the alpha particles is given by

$$dN/dE = E^{1/2} \quad (E_{Max} - E)^2 ,$$

where E_{Max} is the maximum energy available to a single alpha particle in the breakup. This curve, normalized to the total number of alpha particles, together with the experimental energy distribution, is shown in Fig. 4. As can be seen, the agreement is not very good, and it was concluded that the events proceeded by some other mechanism.

Next, the possibility that Be^{8*} was involved as an intermediate nucleus in any of the reactions was investigated. For those events in which the reaction proceeded via Be^{8*}, two of the three alpha particles were produced in the breakup of the Be^{8*}. The vector that connects their end points is a direct measure of the excitation energy (E^*) of the Be^{8*}. Since it is not known which two of the three alpha particles were produced in the breakup of the Be^{8*}, the calculation of E^* was done for each of the three pairs of alpha particles belonging to each event. Thus, only one third of the E^* values obtained are significant. The kinematics of the Be^{8*} breakup are shown on the next page.

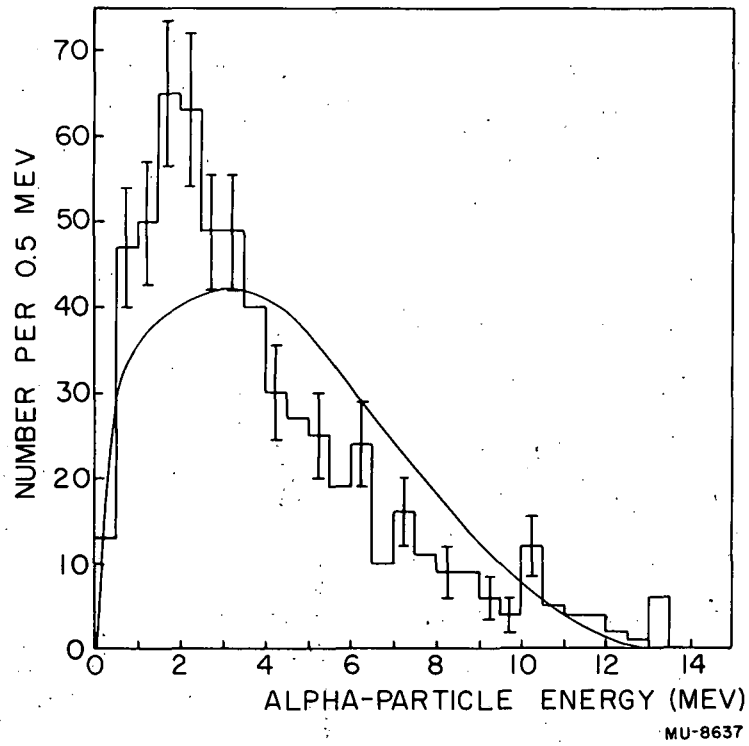

Fig. 4. Total center-of-mass energy distribution for alpha particles. The indicated errors are the statistical standard deviations.

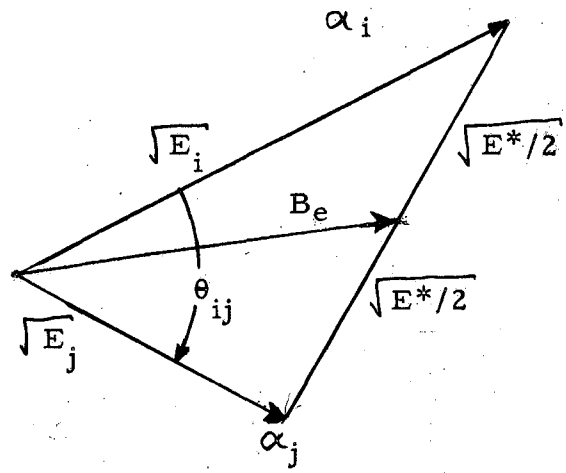

Because the particles of interest are identical, momentum vectors can be used instead of velocity vectors. The unit of momentum is the momentum of a 1-Mev alpha particle. It can be seen that

$$(2\sqrt{E^*/2})^2 = E_i + E_j - 2\sqrt{E_i E_j} \cos\theta$$

or

$$E^* = (E_i + E_j)/2 - \sqrt{E_i E_j} \cos\theta$$

The value $\sqrt{E_i E_j} \cos\theta$ is merely the scalar product of the two vectors representing the momenta of the alpha particles. These relations are correct in any coordinate system.

If all the events, or an appreciable fraction of them, have proceeded via definite levels in Be^8 there will be peaks in the E^* distribution corresponding to the levels involved. Because only one in three of the E^* values is significant, the peaks will be superposed on a continuous background. The E^* distribution for all the events is shown in Fig. 5. There are two marked peaks, one at 0.5 Mev and the other at 3.0 Mev. Of the 51 values of E^* less than 0.5 Mev, 43 lie at 0.1 Mev. The energy available for the breakup of the Be^8 ground state into two alpha particles is 96 kv; therefore the 51 events with one E^* value less than 0.5 Mev are interpreted as having proceeded

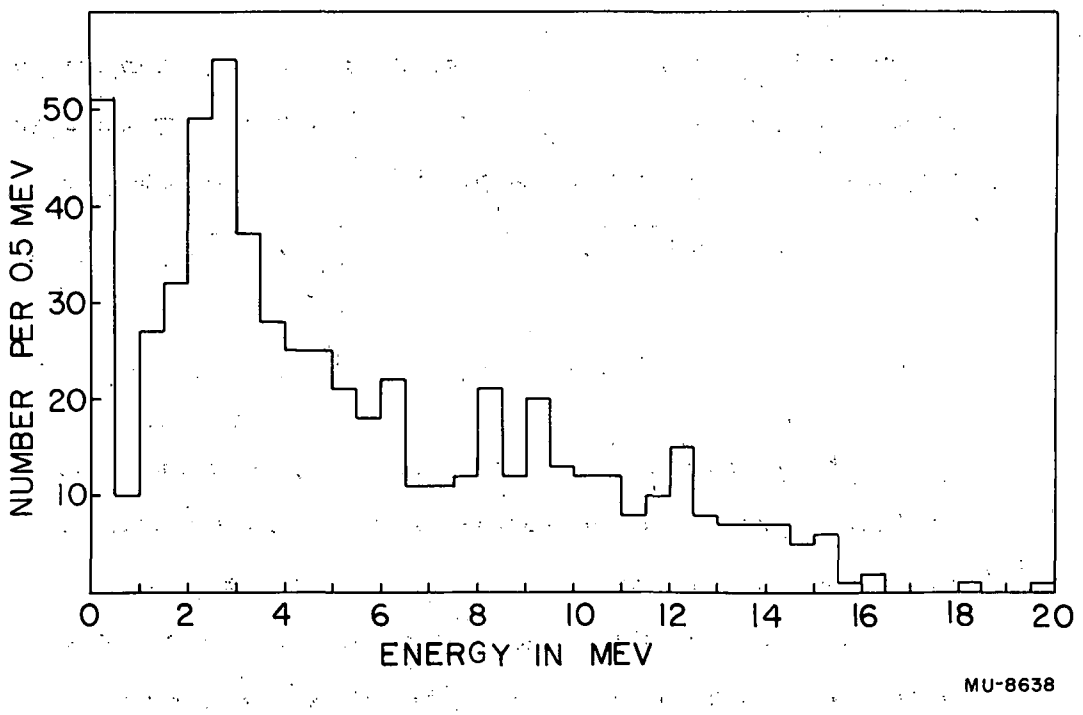

Fig. 5. Total distribution in E*.

via the ground state of Be^8 as an intermediate nucleus. Figure 6 is a picture of an event that was interpreted in this fashion. The two alpha particles below the beam are the two produced in the breakup. There is also a level in Be^8 at an excitation energy of 2.9 Mev[16] which has a width of 1.0 Mev. Some of the E^* values below 0.5 Mev may be due to the extremes of this level, but the probability is only 0.03.

Figure 7 gives the distribution in E^* for those 51 events with one value of E^* below 0.5 Mev which have been interpreted as having proceeded via the ground state of Be^8. This group will be referred to in the future as the Ground State Group. The separation of those values of E^* greater than 0.5 Mev into two groups indicates that the ground state of Be^8 is produced in at least two types of reactions. The group around 2 Mev was produced by reactions in which the proton carried off most of the energy and which probably involved C^{12} excited to a few Mev above threshold as an intermediate nucleus. That group centered at 12 Mev was produced by events in which most of the energy was carried off by one of the alpha particles and involved either C^{12} in highly excited states or the low-lying states of B^9.

In Fig. 8 the E^* distribution for the other 149 events is shown. This group will be referred to in the future as the Three-Mev Group. The peak in the distribution in the vicinity of 3.0 Mev is interpreted as indicating that the great majority of these events went via the broad 2.9-Mev level in Be^{8*}. The indication of a subsidiary peak in the vicinity of 9.0 Mev is similar to that seen by Elder and Telegdi[7] in their study of the $C^{12}(\gamma, 3\alpha)$ reaction with 32-Mev bremsstrahlung. Their interpretation was that possibly higher levels of Be^8 contribute to the reaction. The position of the peak, however, does not agree with the known levels at 7.5 and 10.0 Mev. Statistical fluctuations could account for the presence of this peak.

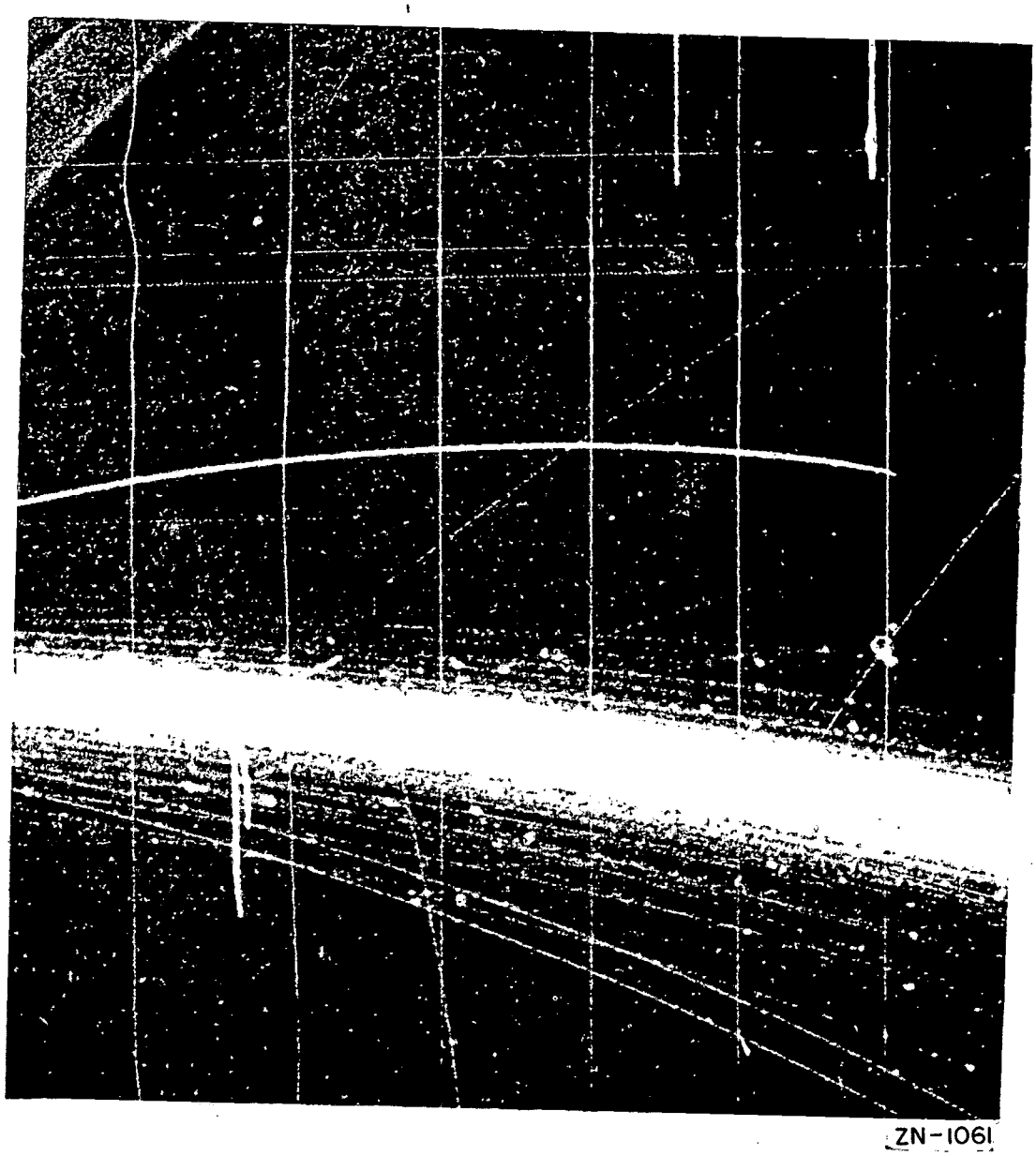

Fig. 6. A photograph of an event in which the ground state of Be^8 was involved. The two alpha particles below the beam were produced by the decay of the Be^8 intermediate nucleus.

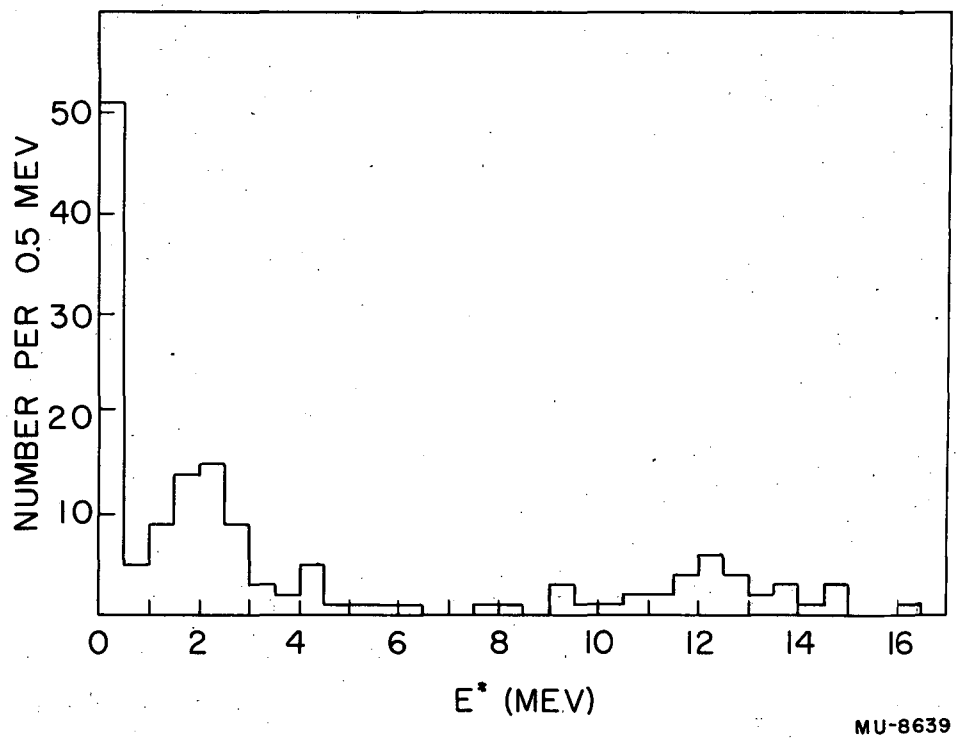

Fig. 7. Distribution in E* for those events with one E* value < 0.5 Mev.

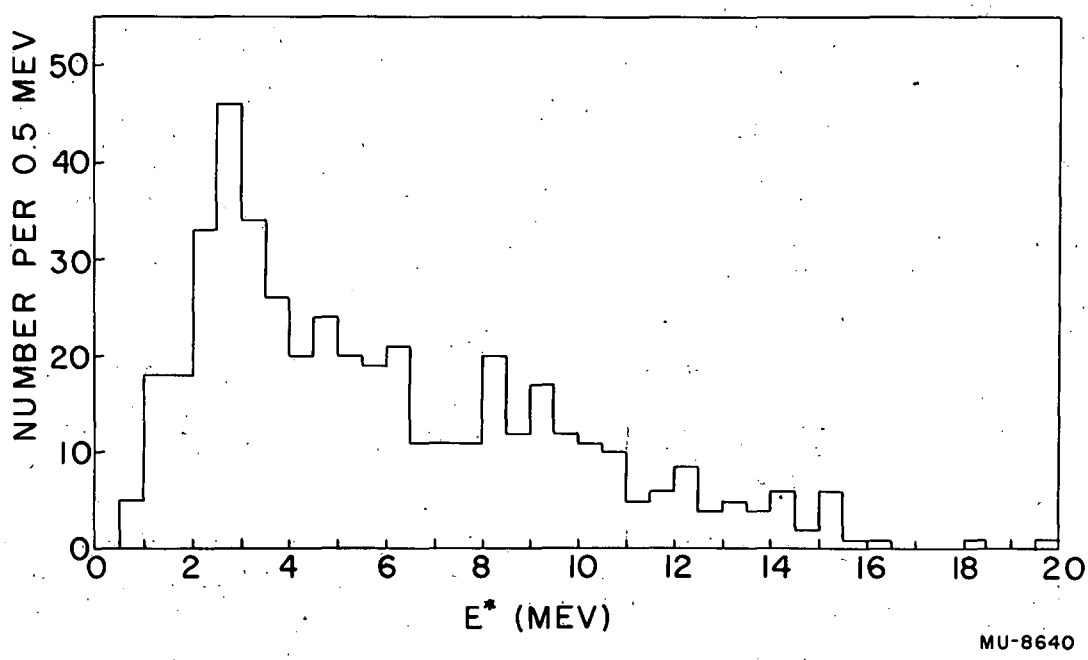

Fig. 8. Distribution in E* for those events with no E* value < 0.5 Mev.

Further evidence for the possibility of the involvement of higher levels in Be^{8*} comes from the fact that 19 events had all E^* greater than 4.5 Mev, but the interpretation of these events remains uncertain. Their E^* distribution shows a peak at about 6.0 Mev. Of these events, 15 are consistent with the $C^{12} + p \rightarrow Li^5 + Be^8$ reaction. The peculiar nature of these 19 events might also be due to errors in measurement; 16 of them had one or more alpha particles which had large errors because of exceptional difficulty in measurement.

The next step in the analysis was to consider all 200 events as though they had proceeded via levels in C^{12*}. The excitation energy of the C^{12} (E_C) can be obtained in two ways: (a) by adding the energies of the three alpha particles in the rest frame of the carbon nucleus to the Q of the $C^{12} \rightarrow 3\alpha$ reaction; and (b) by subtracting 13/12 of the proton energy in the center of mass of the whole system from the total energy available in this center of mass. These two values for the excitation of the C^{12} nucleus should agree within the errors for those events which proceed either through C^{12*} or through states in B^9. The difference between them cannot, therefore, serve to differentiate the two types of events.

For low excitation energies, the three alpha particles stop in the gas (Fig. 6), and the errors in measuring their energies are generally small compared with the error in the determination of the proton energy. On the other hand, for high excitation energies, the error in the proton energy is small compared with the error in the sum of the alpha-particle energies. (Figure 9 shows such an event, with the low-energy proton having stopped in the chamber.) Therefore, three plots were made: (a) $E_C(p)$, calculated from the proton energy; (b) $E_C(\alpha)$, calculated from the sum of the alpha-particle energies in the C^{12*} rest frame; and (c) $\overline{E}_C$, a weighted average of (a) and (b).

Fig. 9. A photograph of an event in which the proton stops in the gas.

The values of $E_c(\alpha)$ and $E_c(p)$ were weighted inversely as the errors in the center-of-mass energy,

$$\bar{E}_c = \left(\frac{E_c(\alpha)}{\Sigma \Delta E_\alpha} + \frac{E_c(p)}{\Delta E_p} \right) \div \left(\frac{1}{\Sigma \Delta E_\alpha} + \frac{1}{\Delta E_p} \right)$$

A straight average was definitely not correct, and the method used had the advantage of being easy to calculate. The errors in the lab energies are not the same as the errors in the center-of-mass energies, but it seemed reasonable to assume that the relative magnitude of the alpha-particle and proton errors was not drastically changed by the transformation. The $\bar{E}_c$ distribution, shown in Fig. 10, was plotted separately for the Ground-State Group and the Three-Mev Group. The events were divided into three main groups as shown, which were then investigated separately.

Group A --$8.0 \leq \bar{E}_c < 13.0$ Mev -- 42 Events

Because all events with $\bar{E}_c < 11.0$ Mev involved the ground state of Be^8, a further division at 11.0 Mev was made. The distributions in $E_c(\alpha)$ and E* are shown in Fig. 11. The short arrows show the kinematic limits of E* and the long arrows show the positions of the peaks to be expected. The limits and the locations of the peaks were calculated for events that went via appropriate levels in C^{12*} and Be^8. The interpretation of these distributions is as follows: Group A_1 -- the events proceeded via the 9.6-Mev level in C^{12} and the Be^8 ground state in a two-step process; Group A_2 --the events went via the levels in C^{12*} in the region from 10.8 to 12.8 Mev to either the ground or first excited levels in Be^8, also in a two-step process, with $43 \pm 17\%$ having gone via the ground state.

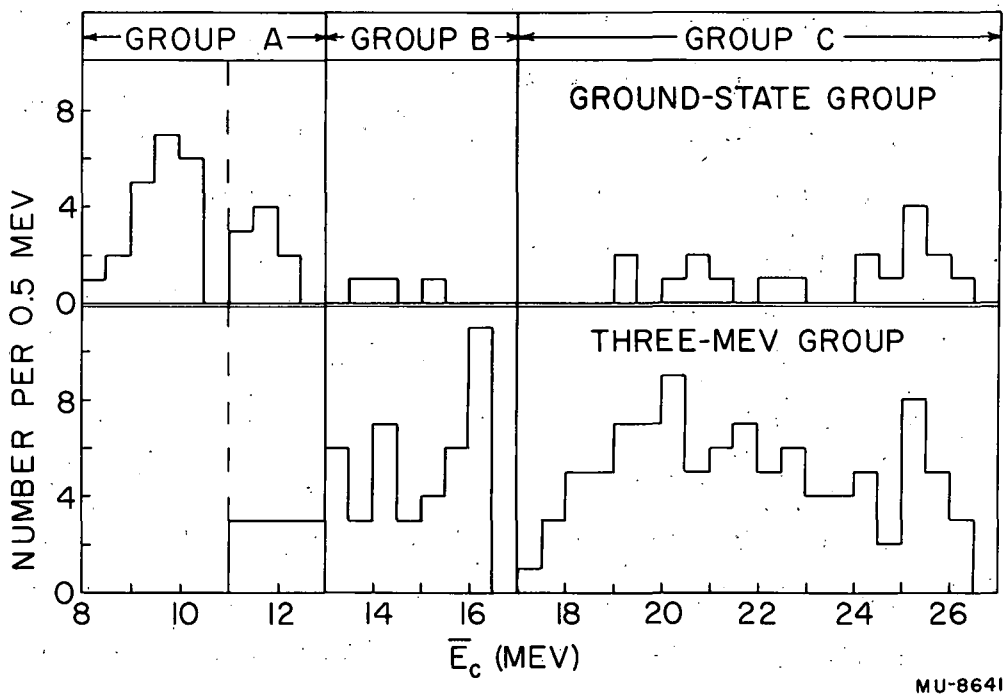

Fig. 10. Distribution in $\overline{E}_c$ for all events.

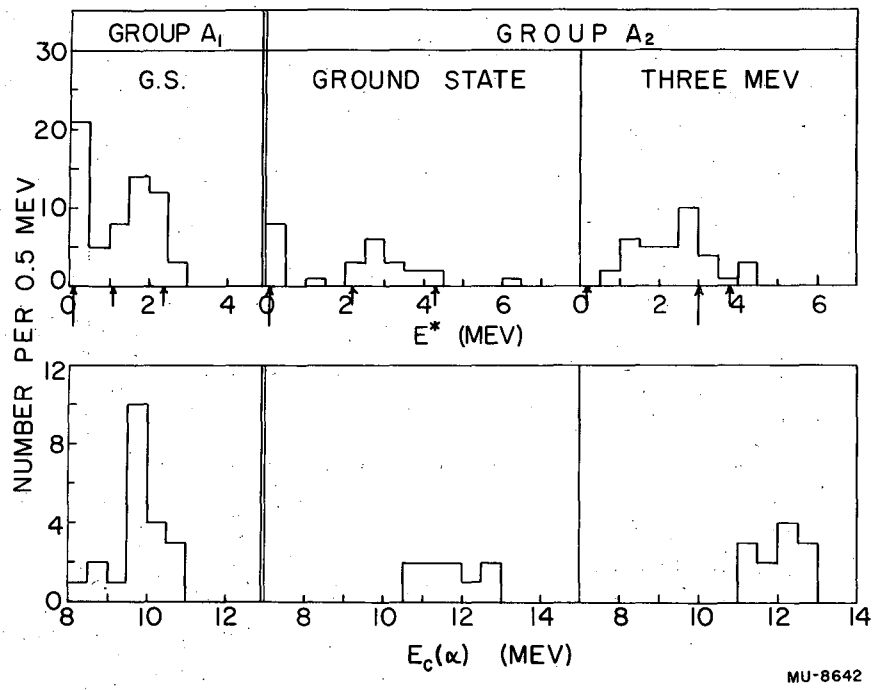

Fig. 11. The distributions in E_c (α) and E* for Groups A_1 and A_2.

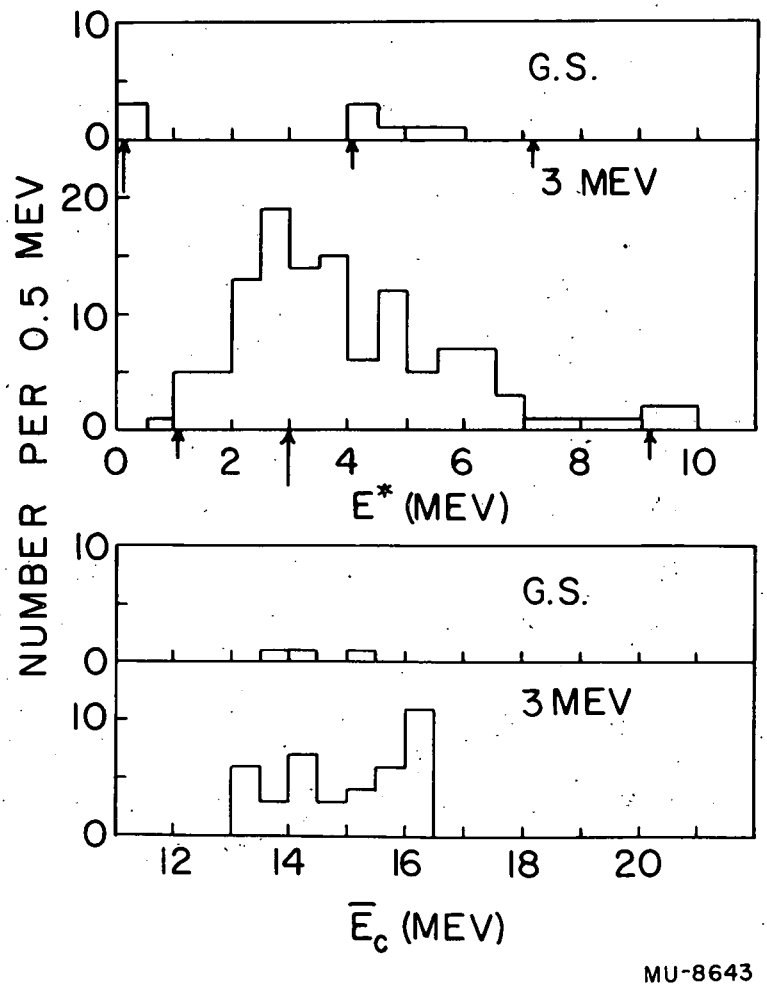

Fig. 12. The distributions in $\bar{E}_c$ and E* for Group B.

Group B--13.0 $\leq \bar{E}_c <$ 17.0 Mev -- 43 Events

The values of $\bar{E}_c$ and E* for this group are given in Fig. 12, separately for the Ground-State and the Three-Mev groups. The $\bar{E}_c$ distribution is fairly smooth, but one might say that the peak at 16 Mev is due to the 16.1-Mev level in C^{12}, which is known to emit alpha particles.[16] This level is the level formed by 163-kv protons on B^{11}, and is the level studied by Dee and Gilbert.[1] The small (7.5 ± 4.5%) involvement of the Be^8 ground state is consistent with the C^{12} (γ, 3 α) results[8] and also the B^{11} (p, α) Be^{8*} data.[2] The rest of the events appear to have gone via the 2.9-Mev level in Be^{8*}.

The assignment of the events in Groups A and B as proceeding via levels in C^{12*} is fairly certain. In Group A, all the alpha-particle energies in the center-of-mass system lie within the kinematic limits. For Group B, four events (out of 43) have alpha particles with energies that lie above the kinematic limits; however, the errors in the energies overlap the limit sufficiently to account for these. Were these higher-energy alpha particles produced directly in (p, α) reactions, they would correspond to B^9 produced in excited levels around 9 to 11 Mev. From the data it is impossible to say that these events are not produced in this fashion. Perhaps a counter experiment with good energy resolution and good statistics could find peaks in this region of the alpha-particle spectrum, which would then be evidence for the B^9 reaction at this excitation.

The events in these two groups were also examined to determine whether they could have been produced by the $C^{12} + p \rightarrow Li^5 + Be^8$ reaction. Only three events (out of 85) could be so interpreted; one of these fits the Li^5 reaction better than the C^{12}. Further, all events in the Groups A and B had one $E^* <$ 4.5 Mev, so that they are consistent with transitions either through the ground state or the first excited level of Be^8.

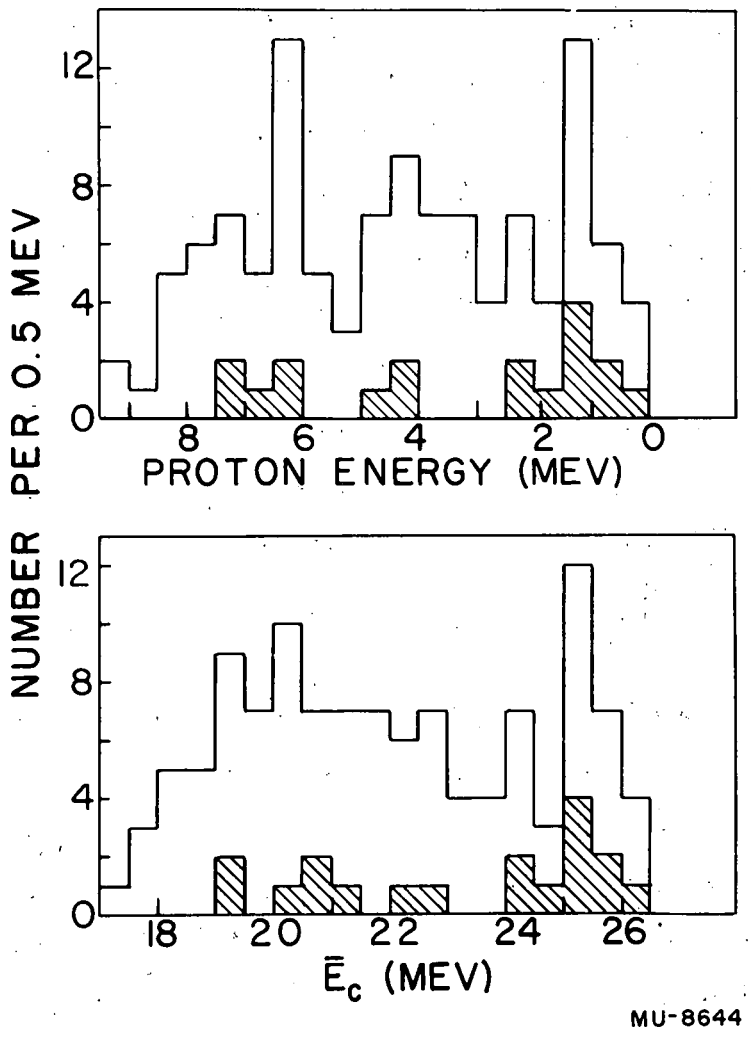

Fig. 13. The distributions in proton energy (E_p) and $\bar{E}_c$ for Group C.

The situation with respect to Group C is more complex. In addition to the C^{12} events, the low-lying levels of B^9 can give $\overline{E}_c$ values in this group as will the $C^{12} + p \rightarrow Li^5 + Be^8$ reaction. Figure 13 shows the distribution of proton energies and the $\overline{E}_c$ distribution for all events in Group C plotted so that corresponding energies lie at the same abscissa. Three subgroups, as shown, were chosen. The crosshatched regions show the distribution for the Ground-State Group. Both distributions show evidence of level structure at C^{12*} with levels at 20 and 25 Mev.

Strauch and Titus[17] report a level at 20 ± 1 Mev produced by inelastically scattered protons of 96 Mev bombarding energy. Hecht[18] reports a level in the vicinity of 19.5 Mev, seen in inelastic scattering of 32-Mev protons. It seems possible that the level at 20 Mev found in this work is the same level reported by these workers.

A resonance at 1 Mev in the B^{10} (d,α) Be^8 reaction has been reported by Whitehead.[19] This corresponds to a level in C^{12} at an energy of 26.3 Mev. Transitions to both the ground state and the first excited level in Be^8 were seen, the ground-state transitions occurring in about 25 percent of the cases. If all the events in Group C_3 are assumed to belong to the resonance, it follows that 27 ± 10 percent went via the ground state. The level at 25 ± 1 Mev seen in this work may possibly be identified with the level reported by Whitehead, or it could be the level seen by Goward and Wilkins[8] at an energy of 25.6 Mev, which decays by α-emission.

The energy resolution and statistics of this experiment are insufficient to separate Group C_2 into any definite levels.

To determine the modes of decay of these levels in C^{12}, distributions in E^* were made for each subgroup separately. The statistics were poor, however. Therefore the total E^* distribution for all the

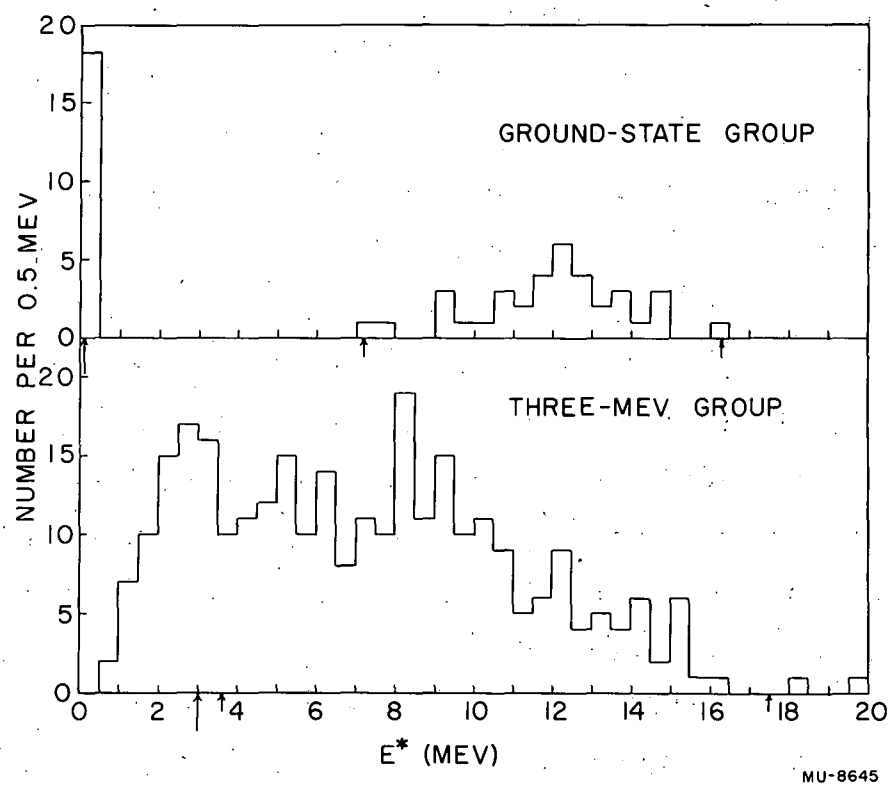

Fig. 14. The distributions in E* for Group C.

events in Group C was plotted. It is given in Fig. 14. The long arrows show the position of the expected peaks and the short arrows the limits of the continuum. These locations were calculated on the assumption that the events were due to C^{12} levels and went via either the 2.9-Mev level or the ground state of Be^{8}. The experimental results agree very nicely for the Ground-State Group. In the case of the Three-Mev Group, however, the agreement is not as good. The slight indication of a peak at 3.0 Mev does not account for enough of the events. It would seem surprising if none of the events went via the 2.9-Mev level, in view of the fact that the ground state participated. From the height of the distribution at 3.0 Mev it is estimated that between one-third and one-half of the events in the Three-Mev Group proceeded via the 2.9-Mev level. The peak in the vicinity of 8.0 Mev is compatible with statistical fluctuations, but it might become more definite with more data. If it is considered to be real then it can be interpreted as indicating that higher levels in Be^{8*}, possibly the 7.5- and 10.0-Mev levels, participated in the reaction from these high levels in C^{12}. The possibility of three-particle breakup is not excluded, and this mechanism could account for as much as one-third of the events in this group.

The above analysis of Group C has been carried out on the assumption that C^{12} levels participated in all the events. It is known[14] that the C^{12} (p,α) B^{9} reaction occurs at 18 Mev bombarding energy, and it is highly unlikely that it does not occur with 29-Mev protons; therefore the assumption that all events proceeded via levels in C^{12} is probably not justified. However, the conclusions about the proportion of events that proceeded via levels in Be^{8} which were made from the E^{*} distribution are not changed. The shape of the E^{*} distribution is chiefly determined by the Be^{8} levels involved, and is only slightly dependent upon the nucleus from which the Be^{8}

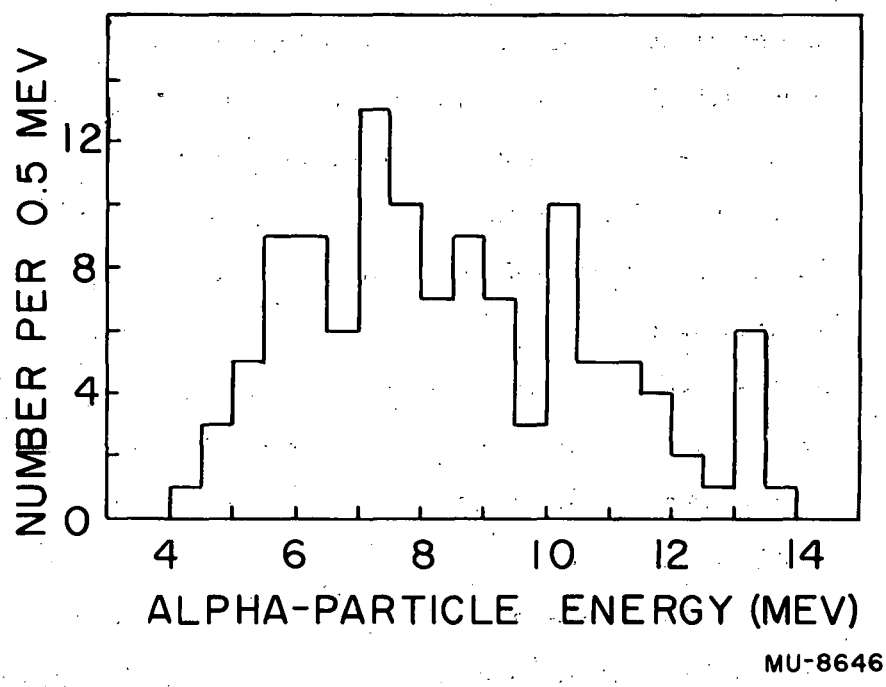

Fig. 15. The distribution in energy of the most energetic alpha particle of each event in Group C.

was formed. When the E^* distribution was calculated for events proceeding via levels in B^9 the results were not sufficiently different to be distinguished with the data on hand.

In order to analyze the data for evidence of the $C^{12}(p,\alpha)B^9$ reaction, a plot was made of the energy distribution of the most energetic alpha particle from each event in Group C. Figure 15 presents the results. The distribution shows evidence for groups at 13 and 10 Mev, which correspond to the ground state, and a level at 4 Mev. There is no evidence for the known level at 2.4 Mev (which would appear at an alpha-particle energy of 11.5 Mev); however, the statistics are not good and the energy resolution is about $\pm$ 1.5 Mev.

As a further examination of the levels of the B^9 reaction, a transformation to the B^9 rest frame was carried out for all the events in Group C. The transformation was effected by adding 4/9 of the velocity components of the most energetic alpha particle to the velocity components of the other three particles. Then the energies of the proton and the two alpha particles in the B^9 rest frame were determined. The sum of these energies was plotted against the energy of the most energetic alpha particle. Only those events which fell within 1.5 Mev in E_α of the expected line were considered. On the basis of calculations, all the events, whether they proceeded via C^{12} or B^9, should lie in this region of acceptance. The grouping in evidence in Fig. 16, however, would come about only if some of the events proceeded via B^9 levels. The combination of the peaks in the energy spectrum of the most energetic alpha particles, together with the grouping in Fig. 16, gives good evidence for the participation of B^9 levels in the reaction. The position of the second group in Fig. 16 is at 3.5 $\pm$ 1.0 Mev. This corresponds to an excitation energy of 3.2 $\pm$ 1.0 Mev for the B^9, which is in better agreement with

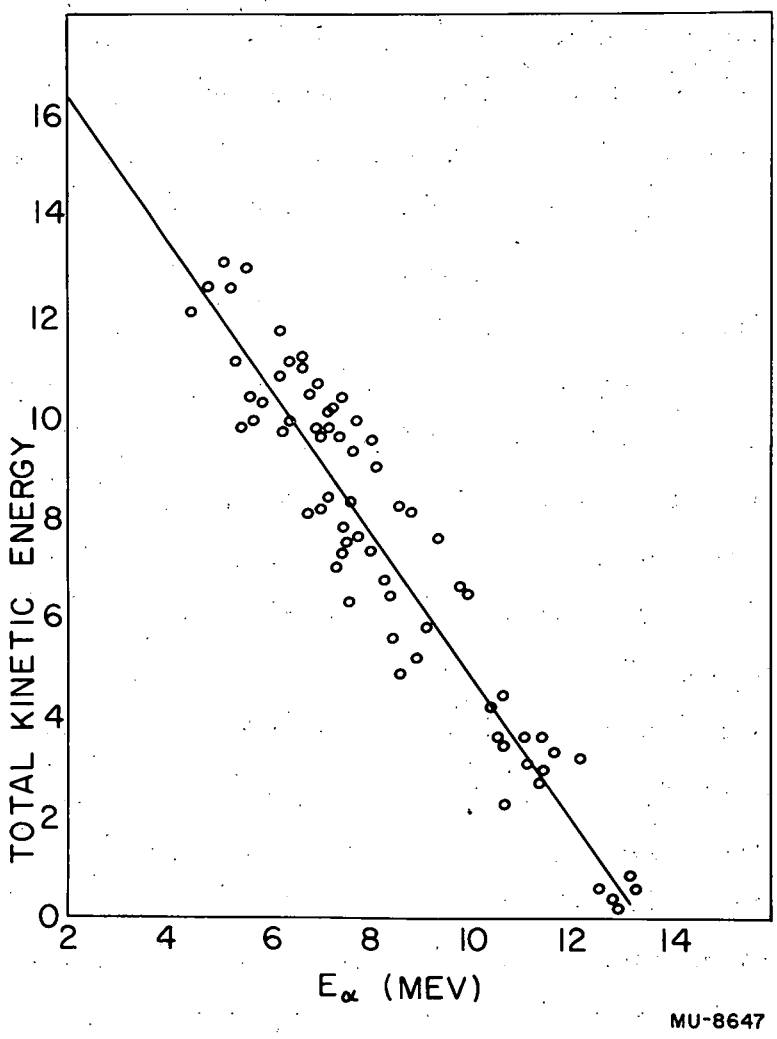

Fig. 16. A diagram with the energy of the most energetic alpha particle of each event as abscissa and the sum of the kinetic energies of the proton and the other two alpha particles in the B^9 rest frame as ordinate for selected events.

the value of 2.4 Mev for the known level. The question of the existence of the energy levels of B^9 certainly needs further investigation.

The question still remains as to the decay mechanism of the B^9. The five events in the B^9 ground-state group have one value of E^* less than 0.5 Mev. However, there is only 0.28 Mev available for the breakup of the ground state of B^9 into two alpha particles and a proton, so that even if the breakup went directly to a proton and two alpha particles there would be one value of E^* less than 0.5 Mev. Thus, the fact that these five events have such a value of E^* is not necessarily an indication that Be^8 in the ground state was involved. Of the twelve events in the second group in Fig. 16, six have one value of E^* less than 0.5 Mev. There is about 3.5 Mev available for the breakup from this level, and the presence of one value of E^* less than 0.5 Mev for an event is good evidence that the Be^8 ground state was involved in the reaction. The other six events in this group are consistent with decay through the other levels of Be^8 in the same proportion as determined by the C^{12} analysis, as are the remainder of the events in Fig. 16.

The last point to be examined is the possibility of the $p + C^{12} \rightarrow Be^8 + Li^5$ reaction. This is a two-body reaction, and therefore the energy of the Be^8 in the center of mass will have one of several unique values, depending on the states in which the Be^8 and Li^5 are formed. Only the ground state and the 2.5-Mev level[16] of Li^5 are accessible with the energy available. The energy of the Be^8 in the center of mass is given by

$$E_{Be} = E_{\alpha i} + E_{\alpha j} - E^*_{ij},$$

or, the sum of the kinetic energies in the center-of-mass system of the two alpha particles produced in the Be^8 decay minus the Be^8 excitation energy. A more convenient value to calculate is the

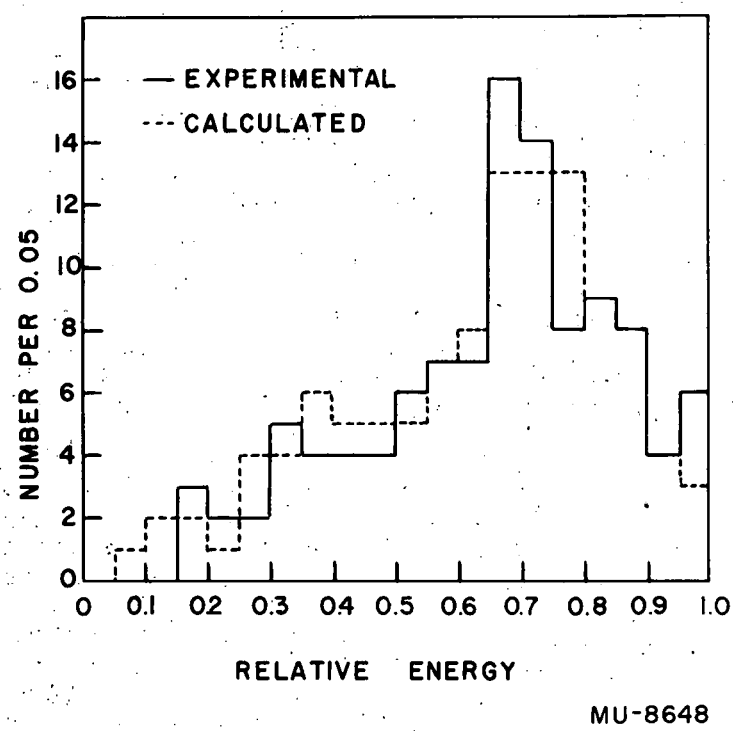

Fig. 17. The distribution in ϵ_{Be} for Group C.

relative energy of the Be^8, ϵ_{Be}. It is given by

$$\epsilon_{Be} = \frac{E_i + E_j - E^*_{ij}}{19.2 - E^*_{ij}} .$$

The value 19.3 Mev is the kinetic energy available to the Li^5 and Be^8 when they are both formed in their ground states. For the ground state of Li^5 the ϵ_{Be} values lie between 0.87 and 0.92, and for the 2.5 Mev Li^5 level, between 0.72 and 0.78. The proper choice of the two alpha particles produced in the Be^8 decay for each event has been facilitated by the E^* determination. The calculation of ϵ_{Be} was carried out for all events. For those events in the Ground-State Group the pair of alphas which produced the low value of E^* were chosen. For the other events, each pair that produced an E^* between 1.5 and 4.5 Mev, or, if none, then that pair which gave the lowest E^* value, was chosen. Only three events (out of 85) in Groups A and B could have proceeded in this fashion. For Group C there are 49 that are consistent with the Li^5 possibility. The ϵ_{Be} distribution from the events of Group C is given in Fig. 17. When there were two ϵ_{Be} values for an event, the choice was made by flipping a coin. Also shown in the figure (dotted line) is the ϵ_{Be} distribution to be expected from the events of Group C if they go via C^{12} in the proportions determined above, normalized to the same number of events. The agreement between the two curves is excellent. The experimental peak at 0.65 Mev is below the peak at 0.75 expected for the Li^{5*} reaction, and there is no evidence for a peak around 0.90 that would be produced in the Li^5 ground state reaction. Therefore, there seems to be no evidence for any large contribution to the events from this reaction with at most five percent of the events having been produced in this fashion.

In summary, there were 51 events with one value of E* less than 0.5 Mev that were interpreted as involving the ground state of Be^8 as an intermediate nucleus. An additional 130 events had one value of E* between 1.0 and 4.5 Mev. This group is consistent with transitions through the 2.9-Mev level in Be^{8*} as an intermediate nucleus. The remaining 19 events had every value of E* greater than 4.5 Mev. It is difficult to assign any definite mechanism to this group. The events could have been due to the participation of higher levels in Be^8, the $C^{12} + p \rightarrow Li^5 + Be^8$ reaction, or the three-particle decay of C^{12}.

Definite evidence for the participation of levels in C^{12} was seen. Levels were identified at 9.6, 11.8, 16, 20, and 25 Mev. The 9.6-Mev level went only to the ground state in Be^8. The levels in the vicinity of 11.8 Mev went to both the ground state and the 2.9-Mev level of Be^8 with equal probability. For the events which included the 16-Mev level in C^{12} less than 5% went to the Be^8 ground state and the rest were consistent with transitions to the 2.9-Mev level in Be^{8*}. The decay mechanism of the 20- and 25-Mev levels is uncertain because a given event could equally well be interpreted as having proceeded in one of several ways. For these two levels the identification of the 18 events that proceeded via the ground state of Be^8 was good, the identification of those that went via the 2.9-Mev level in Be^{8*} was doubtful. It was estimated that about one-third of the events that involved the 20- and 25-Mev levels and that did not go via the Be^8 ground state (97 events) proceeded via the 2.9-Mev level in Be^{8*}. The mechanism in the remaining events was undecided.

The investigation of the possibility of the B^9 reaction showed that the ground state and first excited state of B^9 were produced and decayed into two alpha particles and one proton. The mechanism of the decay of these levels was undecided though some of the events

were consistent with the participation of the ground and 2.9-Mev levels of Be^8. Because of the inability to assign an event uniquely to a given reaction no estimation of the relative cross section was made.

The reaction $C^{12} + p \rightarrow Li^5 + Be^8$ was investigated and it was found for all events that although 43 of the events, all in Group C, were consistent with this reaction, the distribution in relative energies of the Be^8 nuclei was fitted by the distribution to be expected from the events in Group C when considered as having proceeded via the levels in C^{12}. It was estimated that this reaction could account for no more than 5% of the events.

ACKNOWLEDGMENTS

It is a pleasure to express my sincere gratitude to Professor Wilson M. Powell and Dr. Theodore C. Merkle for their helpful advice and constant encouragement throughout the investigation. The cooperation of many members of the cloud chamber group is also acknowledged, especially that of Dr. Arthur Wickersham and Mr. Oscar Kolar, who assisted during the design and preparation of the experimental arrangement and worked many nights during the runs.

I am indebted to Mr. Howard White and Mr. H. B. Knowles for helpful discussions about the calculations and analysis. Thanks are also due my wife, Irene, Mr. Vincent Arp, and Miss Barbara Schultz for their assistance in the tedious work of the calculations.

This work was performed under the auspices of the Atomic Energy Commission.

APPENDICES

I. Range-Energy Relation

The range-energy relation was desired for ion velocities below the velocity of the electrons in the k-shells, i.e., in the region where the relative stopping powers of various gases vary with energy. With a mixture of gases in the chamber, the only way to get an accurate range-energy relation is to determine the stopping power of the mixture for protons and alpha particles as a function of energy and then to integrate numerically the resultant curves. The data on stopping powers of various gases for protons and alpha particles were found in the articles of Livingston and Bethe,[20] Hirschfelder and Magee,[21] Bethe,[22] and Allison and Warshaw.[23]

At the conclusion of each run the temperature of the chamber was recorded. The pressure in the expanded chamber and the barometric pressure were measured with a mercury manometer. A sample of the gas in the chamber was taken and analyzed with a mass spectrograph. The mass spectrograph does not measure the water-vapor concentration with any degree of reliability; therefore the water-vapor pressure was determined from the temperature. With these data the percentage compositions of the several gas mixtures were computed. A typical sample had 4.8% water vapor, 67.3% methane, 26.8% hydrogen, and 1.1% air.

Using the percentage compositions, the temperature, pressure, and the tabulated values of $E\sigma_H$, $E\sigma_C$, and $E\sigma_O$ of Hirschfelder and Magee (where σ is computed in units of ev cm^2 x 10^{15}/atom), the values of dx/dE in cm/Mev were computed for protons in one mixture, for values of the energy between 0.01 and 3.00 Mev. These values are theoretical ones. From the same gas data and from σ_{H_2O}, σ_{CH_4} and σ_{H_2} found in Allison and Warshaw, dx/dE was

computed for protons in the same mixture for values of the energy between 0.03 and 0.60 Mev. These values are based on experimental work. The two curves matched at 0.60 Mev. The data in Allison and Warshaw were used for $E \leq 0.60$ Mev, and those of Hirschfelder and Magee for $E >$ 0.60 Mev. The curve was then plotted and was integrated by square-counting below 0.10 Mev and by trapezoidal integration above. The range of 0.03 Mev was assumed to be the range in air of a 0.03-Mev proton divided by 0.214. It had a value of 0.281 cm. For comparison, the range at 0.50 Mev was 3.164 cm. The number 0.214 is a mean value for the relative stopping power of the mixture and air in the region from 0.03 to 0.10 Mev. The error in the integration was less than 0.6%, and the experimental error in the values of the stopping cross sections was about 3%.

As a check on the integration, the integrated curve was multiplied by a constant to give the best fit to the range-energy curve for protons in air for energies up to 2.0 Mev. (A 2.0-Mev proton leaves the chamber.) The two curves were matched at 1.00 Mev. The error is everywhere less than 0.05 Mev, and the percent error is a maximum of 10% at 0.50 Mev. At this energy the range is 2.5 cm and the percent error in range due to uncertainty in origin is 8%.

To determine the range-energy relation for alpha particles in the mixture it was necessary to convert in some fashion the values of the stopping power of the mixture for protons to stopping powers for alphas, since the only available data were for alpha energies between 0.03 and 0.10 Mev. It is known that for ion velocities above the velocity of the k-shell electrons $4\sigma_p = \sigma_\alpha$ when they are compared at equivalent energies, $E = E_\alpha/4 = E_p$. Below this critical velocity anything can happen. To get an idea of what does happen, the value of $4\sigma_p/\sigma_\alpha$ at equivalent energies was plotted from

the small amount of experimental data given in Allison and Warshaw over the available energy range. The gases for which this was done were air, hydrogen, helium, and argon. Also plotted on the same graph was the value of $4\sigma_p/\sigma_\alpha$ for air in the energy region between 0.03 and 0.60 Mev from the data of Livingston and Bethe. This value goes to one at 0.60 Mev. There was a discrepancy between the two sets of data for air. To decide which to use, the values of σ_p for air from the two articles were plotted. Again a discrepancy was noted, but it was in such a direction as to be consistent with the discrepancy in the $4\sigma_p/\sigma_\alpha$ data. Because the data in Allison and Warshaw are more recent and are experimental, more weight was given to those curves than to that of Livingston and Bethe in drawing the final curve. The values of $4\sigma_p/\sigma_\alpha$ were taken from the curve for those energies for which σ_p was available and were used to calculate the values of dx/dE for alphas in the mixture. These were plotted and graphically integrated. The resultant range-energy curve for alpha particles in the mixture was then multiplied by the factor determined from the proton best fit and compared with the range-energy curve for alphas in air.[22] The largest deviation was 0.14 Mev. The error was a maximum of 8% at 2.5 Mev.

The same procedure was followed for the second mixture. When the integrated range-energy curve for protons in this mixture was fitted by a multiplicative constant to the range-energy curve for protons in Mixture One at 1.00 Mev, the two curves matched within 0.01 Mev over their entire length. When the integrated range-energy curve for alpha particles in this second mixture was multiplied by the <u>same</u> constant it matched the range-energy curve for alpha particles in Mixture One to within 0.02 Mev!

In order to save time, the third mixture was treated differently. Only the proton curve was integrated, and it was done only to 1.00 Mev. The ratio $R^{(3)}_p(1.00)/R^{(1)}_p(1.00)$ was determined and used as a multiplicative factor to get both the proton- and alpha-particle range-energy curves in the third mixture from the corresponding curves in Mixture One.

The range of a 1-Mev proton in a gas was obtained by multiplying the range of a 1-Mev proton in Mixture One by the number obtained when the sum of the stopping powers of that gas for protons of 0.1 and 1.0 Mev was divided by the corresponding sum for Mixture One. It was found that this procedure was valid for the two mixtures that were integrated, and it was then used to compute the range-energy relations for the remaining two mixtures.

The final range-energy relations are considered to be accurate to within $\pm 5\%$. This includes errors due to experimental errors in the stopping cross sections, errors in the integration, and errors in the temperature and pressure measurements. As a check, the average energies for all the four-prong events were determined for each mixture. Table I shows the results. The over-all average energy when added to the Q (7.3 Mev) of the reaction gave 29.2 Mev, in excellent agreement with the beam energy of 28.9 ± 0.5 Mev. No significant difference was noted between those events where only one prong energy had been measured by range and those where three prong energies had been so measured. The high energy for Mixture Four is due to three cases where only one prong was measured by range.

Table I

Mixture	0	1	2	3	4
$\bar{E}$	21.82	21.95	21.93	21.48	23.49
N	69	13	44	15	8

II. Beam Energy

The mean energy of the proton beam in the cloud chamber was determined by measuring the curvature of the tracks of individual protons as they crossed the chamber and by determining the average magnetic field. During each run, pictures were taken which showed less than twenty protons. These pictures were used for the beam-energy determination.

The projection apparatus (Fig. 2) was used to measure the curvature. After the translucent screen was adjusted to the height of a track, the measurements were made using only one picture. One of several circular arcs ruled on a lucite template was matched to the curve. The arcs were 20 cm long and ranged in radius from 114 cm to 121 cm in steps of 1 cm. The template was then fastened to the translucent screen so that the chosen arc was tangent to the line BB at O. The screen was moved so that O was at a point along the track and then rotated about a vertical axis until the track and the arc coincided. The angle β_B and the arc length S (measured from the same arbitrarily fixed point as was used in measuring the "origin" of each event) were recorded for 14 points along the beam. A plot of S vs β_B for each track yielded points that could be fitted with a straight line within the measurement errors. For a given track, the slope of the straight line is related to the radius of curvature of the track by the formula: $\rho = \Delta S / \Delta \beta \times 180/\pi$. The slope of the straight line for each track was determined by taking the average of the slopes of the lines drawn between the first and the eighth (N/2 + 1); the second and ninth (N/2 + 2), etc. The reciprocal of the sum of the squares of the residuals was used as the weighting factor in determining the final average radius for each value of the magnet current used.

Since the field varied throughout the chamber, the next thing to be determined was the proper space-average value of the magnet field to be used to get the $B\rho$ for the beam protons. The plan used was to calculate the angle of the proton at several points along its path for known magnet current and known energy. These values of S and β_B were then to be treated in exactly the same fashion as the measured values from the projection apparatus. A mean value for the radius was to be obtained which then could be divided into the known $B\rho$ for the proton to yield the proper value for the average field. Three calculations were carried out. The beam, from the center to one edge of the chamber, was divided into five, six, and seven segments respectively. The lengths of these segments were measured on a full-scale drawing. The average value of the field over each segment was taken to be the field at the center of the segment. A magnet current of 2200 amp was assumed. The radius of curvature applicable to each segment was obtained by dividing the known $B\rho$ of a 28.0-Mev proton by the field determined for that segment. Starting at the center of the chamber, the angular deviation of the beam was determined from the length of the first segment and the radius of curvature appropriate to that segment. Also the rectangular coordinates of the end point of this segment were calculated. Then the location of the next center of curvature was found, the next angular deviation, and the rectangular coordinates of the end of the second segment were calculated. The calculation was continued in this stepwise fashion. Using the three sets of angle and arc values so determined, six values of the radius of curvature were determined by using each set with itself and then in pairs. The final result was that the value of the space-average field divided by the field at the center was equal to 0.979 ± 0.003.

The measurements made in this experiment led to a value of 28.6 ± 0.5 Mev for the beam energy. This result was based on the measurement of 58 tracks. Because of the importance of the beam-energy determination and a certain bias on the part of the author during the later measurements, it seemed desirable to have the determination carried out by someone who did not know in advance what results were expected. Very painstaking readings were made on eighteen selected tracks. Eleven of these were accepted for computation. The results obtained yielded a value of 29.1 ± 0.5 Mev for the beam energy, in agreement with the author's results. The final value used was 28.9 ± 0.5 Mev.

The values of the beam energy obtained for the different days did not vary appreciably. The results are shown below.

Table II

Date	9/23	9/28	10/15	11/3	11/6
$\bar{E}$ (Mev)	28.9±0.3	28.3±0.3	28.4±0.3	28.6±0.3	28.7±0.4

REFERENCES

1. P. I. Dee and C. W. Gilbert, Proc. Roy. Soc. 154, 279 (1936)
2. H. A. Bethe, Revs. Modern Phys. 9, 217 (1937)
3. H. Hänni, V. L. Telegdi, and W. Zünti, Helv. Phys. Acta 21, 203 (1948)
4. V. L. Telegdi and W. Zünti, Helv. Phys. Acta 23, 745 (1950)
5. F. K. Goward, V. L. Telegdi, and J. J. Wilkins, Proc. Phys. Soc. 63A, 402 (1950)
6. J. J. Wilkins and F. K. Goward, Proc. Phys. Soc. 64A, 201 (1951); 64A, 1056 (1951); 66A, 661 (1953)
7. M. Elder and V. L. Telegdi, Helv. Phys. Acta 25, 55 (1952)
8. F. K. Goward and J. J. Wilkins, AERE Report GM/127 (1952); Proc. Phys. Soc. 217A, 357 (1953)
9. D. L. Livesey and C. L. Smith, Proc. Phys. Soc. 66A, 689 (1953)
10. C. H. Miller and A. G. W. Cameron, Can. Jour. Phys. 31, 723 (1953)
11. S. D. Softky, "Photodisintegration of C^{12} by 300-Mev Bremsstrahlung", University of California Radiation Laboratory Report No. UCRL-2753, October 8, 1954.
12. H. Aoki, Proc. Phys. Math. Soc. Japan 20, 755 (1938)
13. L. L. Green and W. M. Gibson, Proc. Phys. Soc. 62A, 296 (1949)
14. J. B. Reynolds, Private communication.
15. K. Breuckner, W. Hartsough, E. Hayward, and W. Powell, Phys. Rev. 75, 555 (1949).
16. F. Ajzenberg and T. Lauritsen, Revs. Modern Phys. 24, 321 (1952)
17. K. Strauch and F. Titus, Phys. Rev. 94, 785 (1954)
18. G. Hecht, Private communication.
19. W. D. Whitehead, Phys. Rev. 82, 553 (1951)
20. S. Livingston and H. A. Bethe, Revs. Modern Phys. 9, 261 (1937)
21. J. O. Hirschfelder and J. L. Magee, Phys. Rev. 73, 207 (1948)
22. H. A. Bethe, Rev. Modern Phys. 22, 213 (1950)
23. S. K. Allison and S. D. Warshaw, Revs. Modern Phys. 25, 779 (1953)